Proteomic changes in the extracellular environment of sea bass thymocytes exposed to 17α-ethinylestradiol in vitro

Catarina Moreira, Julie Hétru, Matthieu Paiola, Aurélie Duflot, Philippe Chan, David Vaudry, Patrícia I.S. Pinto, Tiphaine Monsinjon, Thomas Knigge

Version of Record: https://www.sciencedirect.com/science/article/pii/S1744117X21001234
Manuscript_5bbcaba183d7246b61461072ae048196

Proteomic changes in the extracellular environment of sea bass thymocytes exposed to 17α-ethinylestradiol *in vitro*

Catarina Moreira[1], Julie Hétru[1], Matthieu Paiola[1,2], Aurélie Duflot[1], Philippe Chan[3,6], David Vaudry[3,4,6], Patrícia I.S. Pinto[5], Tiphaine Monsinjon[1], Thomas Knigge[1,*]

[1] Normandie Univ, UNILEHAVRE, FR CNRS 3730 SCALE, UMR-I 02 Environmental Stress and Aquatic Biomonitoring (SEBIO), F-76600, Le Havre, France
[2] Department of Microbiology and Immunology, University of Rochester Medical Center, 14642, Rochester, NY, United States
[3] Normandie Univ, UNIROUEN, PISSARO Proteomic Facility, IRIB, F-76820 Mont-Saint-Aignan, France
[4] Normandie Univ, UNIROUEN, Neuronal and Neuroendocrine Differentiation and Communication (DC2N), Inserm U1239, 76821 Mont-Saint-Aignan
[5] Centro de Ciências Do Mar (CCMAR), Universidade Do Algarve, 8005-139, Faro, Portugal
[6] Normandie Univ, UNIROUEN, Institute for Research and Innovation in Biomedicine (IRIB), F- 76183 Rouen, France

*Corresponding author: Thomas KNIGGE
Unité Stress Environnementaux et Biosurveillance des milieux aquatiques, UFR Sciences et Techniques, Université Le Havre Normandie, 25 rue Philippe Lebon, 76063, Le Havre, France. E-mail address: thomas.knigge@univ-lehavre.fr

Key-words: Secretome; immune system; thymus; endocrine disruptor; *Dicentrarchus labrax*

Abstract: The thymus is an important immune organ providing the necessary microenvironment for the development of a diverse, self-tolerant T cell repertoire, which is selected to allow for the recognition of foreign antigens while avoiding self-reactivity. Thymus function and activity are known to be regulated by sex steroid hormones, such as oestrogen, leading to sexual dimorphisms in immunocompetence between males and females. The oestrogenic modulation of the thymus function provides a potential target for environmental oestrogens, such as 17α-ethynylestradiol (EE2), to interfere with the cross-talk between the endocrine and the immune system.

Oestrogen receptors have been identified on thymocytes and the thymic microenvironment, but it is unclear how oestrogens regulate thymic epithelial and T cell communication including paracrine signalling. Much less is known regarding intrathymic signalling in fish. Secretomics allows for the analysis of complex mixtures of immunomodulatory signalling factors secreted by T cells. Thus, in the present study, isolated thymocytes of the European sea bass, *Dicentrarchus labrax*, were exposed *in vitro* to 30 nM EE2 for four hours and the T cell-secretome (*i.e.*, extracellular proteome) was analysed by quantitative label-free mass-spectrometry. Progenesis revealed a total of 111 proteins differentially displayed between EE2-treated and control thymocytes at an α-level of 5% and a 1.3-fold change cut off (n=5-6).

The EE2-treatment significantly decreased the level of 90 proteins. Gene ontology revealed the proteasome to be the most impacted pathway. In contrast, the abundance of 21 proteins was significantly increased, with cathepsins showing the highest level of induction. However, no particular molecular pathway was significantly altered for these upregulated proteins. To the best of our knowledge, this work represents the first study of the secretome of the fish thymus exposed to the environmental oestrogen EE2, highlighting the impact on putative signalling pathways linked to immune surveillance, which may be of crucial importance for fish health and defence against pathogens.

1. Introduction

Vertebrate immunity relies on the two pillars of the innate and the adaptive immune response. The adaptive—or acquired—immune response comprises specialised immune cells, the B lymphocytes of the humoral and the T lymphocytes of the cellular immunity. To this end, B and T lymphocytes are 'educated' in the primary lymphoid organs, *i.e.*, the bone marrow—or its equivalent the head kidney in fish—and the thymus (Litman et al., 2010; Boehm and Swann, 2014).

The thymus is the central lymphoid organ in which the maturation, differentiation and selection of the various T cell subpopulations is accomplished. Thymopoiesis, *i.e.*, the development of the T cell lineage, is composed of distinct sequential steps including the entry of early thymic progenitor (ETP) cells, their proliferation and maturation into CD4+CD8+ double-positive thymocytes followed by positive selection in the thymic cortex, the relocation of maturing thymocytes to the thymic medulla where they undergo negative selection, and, eventually, the egress of mature, self-tolerant T cells from the thymus to the peripheral lymphoid organs (Boyd et al., 1993, Takahama, 2006; Gameiro et al., 2010; Klein et al., 2014). This maturation and selection process requires a microenvironment composed of the so-called thymic stromal cells, which allows for intimate cell surface contacts between the different stromal cells and the developing thymocytes (van Ewijk et al., 2000; Manley et al., 2011; Farley et al., 2013). Thymic stromal cells, which can include all non-T lineage cells, such as thymic epithelial cells (TECs), endothelial cells, mesenchymal/fibroblast cells, dendritic cells, and B cells, provide signals that are essential for thymocyte development, 'instructing' them to proliferate, to differentiate or to die. On the other hand, developing thymocytes provide the necessary signals to induce thymic ontogeny and stromal differentiation (van Ewijk et al., 1994; Anderson and Takahama, 2012). Importantly, this bidirectional 'cross-talk' between developing thymocytes and TECs is also essential for maintaining compartmentalisation into cortex and medulla as well as cellular thymic architecture (Klug et al., 2002; Ribeiro et al., 2013). Developmental arrest of ETPs leads to severe thymus atrophy due to a disorganisation of the stromal compartment in which TECs revert from the unique three-dimensional meshwork through which the thymocytes migrate during their development to a two-dimensional epithelial layout (Klug et al., 2002; Holländer et al., 2006). Indeed, the involuted thymus is marked by alterations in epithelial cell composition and function, as well as fibrosis and adipogenesis (Chaudhry et al., 2016), those alterations within the thymic microenvironment being mainly due to the declining communication between thymic stromal cells and developing thymocytes (Lepleitier et al., 2015).

Primarily, the female sex steroid oestrogen controls reproductive functions. Vertebrate sex steroid hormones have, however, pleiotropic functions in neurological, cardiovascular and skeletal systems (Shved et al. 2008, Froehlicher 2009, Ivanowicz et al. 2009, Segner et al. 2013). Sexual dimorphisms in the efficacy of the immune defence of males and females illustrate the potentially immunosuppressive and immunostimulatory actions of sex steroids (Molloy et al., 2003; Straub, 2007). Notably, oestrogens are known to modulate thymus ontogeny and thymic plasticity (Straub, 2007; Hince et al., 2008). Indeed, Staples *et al*. (1999) demonstrated that oestrogen receptors (ERs) are necessary for correct thymus ontogeny, which has also been demonstrated in fish (Szwejser et al., 2017; Paiola et al., 2017). Consequently, Selvaraj *et al*. (2005) described several 17 β–oestradiol (E2)-responsive genes in thymocytes that were regulated during T cell maturation and selection. Several studies reported that treatment with compounds that exert oestrogenic activity inhibited thymocyte development. Novotny *et al*. (1983) and Gould *et al*. (2000) found that oestradiol or diethylstibestrol inhibited the proliferation of thymocytes, respectively; Rijhsinghani *et al*. (1996) reported that oestrogen blocked the development of ETPs; Mor *et al*. (2001), Okasha *et al*. (2001) and Yao and Hao (2004) demonstrated that oestradiol induced pathways that led to increased apoptosis of thymocytes. Hareramadas and Rai (2006) as well as Zoller and Kersh (2006) confirmed the inhibition of ETPs and proliferation of β–selected thymocytes by oestrogen. Generally, the described effects of oestrogenic action resulted in dramatic reduction of thymus size and cellularity (Martín et al., 1994). Conceivably, oestrogenic blocking of thymocyte development, notably at the stage of ETPs, misses the signals necessary to maintain the thymic architecture,

reduces the regeneration of TECs and, eventually, leads to a disorganised thymic microenvironment. Contrariwise, blocking ETPs prior to important developmental checkpoints in the double negative 3 (DN3) stage could lead to temporary and partial thymus hyperplasia, notably in the cortex (Forsberg, 1996; Okasha et al., 2001; Seemann et al., 2015).

Changes of thymic cellularity and activity occur physiologically throughout life, notably during aging and are characterized by a continuous reduction of the thymic cellular microenvironment (Boehm and Swann, 2013). Thymus involution in mammals also occurs during pregnancy after which the thymus is regenerated (Tibbetts et al., 1999). In many non-mammalian taxa, such as fish, reptiles and birds, a seasonally regulated thymic plasticity can be observed (Nakanishi, 1986; Hareramadas and Rai, 2006; Swejser et al., 2016), which is likely to derive from a trade-off between energetically costly immune and reproductive functions (Cockburn, 1992; Kernen et al., 2020; Paiola et al., 2021). Thymus plasticity related to both, aging and reproductive fluctuations has been associated with changes in hormone levels (Seiki and Sakabe, 1997; Hince et al., 2008; Bodey et al., 2004), and, notably, the role of oestrogen in thymus atrophy has been extensively studied. This has led to the idea that xenoestrogens could act on thymus ontogeny and thymic function of fish (Seemann et al., 2015; Paiola et al., 2018; Moreira et al., 2021). Indeed, Seemann *et al*. (2015) found a significantly decreased thymus volume in juvenile sea bass, *Dicentrarchus labrax*, exposed at 60 days post hatch (dph) to 200 $ng \cdot L^{-1}$ of E2 for 56 days, but detected an increase in the volume of the cortex when 90 dph sea bass were exposed to 20 $ng \cdot L^{-1}$ E2 for the same duration. Paiola *et al*. (2018) reported sex-dependent expression of genetic markers for T cell homing, maturation and selection when sea bass was treated with E2. Moreira *et al*. (2021) observed an effect of 20 $ng \cdot L^{-1}$ E2 on the proliferation and migration of innate-like γδ T cells, which were reduced in peripheral immune organs. It remains, however, largely unclear how the developing thymocytes directly respond to oestrogens. It has been suggested that E2 acts on apoptosis of thymocytes by inducing FasL (Mor et al., 2001), but Zoller and Kersh (2006) could not confirm increased apoptosis in mice after E2-treatment and suggested that the colonisation of the thymus by ETPs or the proliferation of DN3 and DN4 cell stages were affected. A reduction of ETP-entry could not yet be confirmed for fish, but modification of TEC-function was observed in E2-treated *D. labrax*, suggesting negative effects on thymocyte maturation (Paiola et al., 2018). How oestrogens modulate the interactions between the developing thymocytes and the stroma remains an open question.

In part, the signalling between thymocytes and TECs is known (reviewed in Takahama, 2006). It involves cytokines and factors such as notch-mediated signals, IL-7 expressed by TECs, receptor activator of NF-κB (RANK) ligand expressed by CD4+ thymocytes and CD40 (Roberts et al., 2009; Anderson et al., 2009; Ribeiro et al., 2013), and may also involve autocrine or paracrine factors, such as neurotrophins (Linker et al., 2015). Many other elements of this crosstalk are, however, still to be discovered. Especially, it is largely unknown how endogenous and exogenous oestrogens may modulate cell-to-cell communication. As oestrogens are known to modulate cytokines in mammals and exposure to exogenous oestrogen in fish decreased cytokines such as IL-1β and TGF-β, it is conceivable that xenoestrogens modulate autocrine and paracrine signalling of thymocytes and, thereby, affect TECs and the thymic stromal compartment. Because the cellular communication of developing thymocytes is unknown for the most part, especially if it comes to non-mammalian species, we used a global secretomic approach (Mukherjee and Mani, 2013; Wetie et al., 2013) to identify peptides and proteins released by a thymocyte-enriched cell culture fraction into the extracellular space. For this, thymocytes were stimulated *in vitro* with 30 nM 17α-ethynylestradiol (EE2), in order to obtain information regarding the extracellular proteome of developing thymocytes in response to oestrogens and how this is potentially modified when confronted with xenoestrogens.

2. Materials and Methods

2.1. Animals rearing and sampling

European sea bass, *Dicentrarchus labrax*, fingerlings were obtained from the hatchery 'L'écloserie marine de Gravelines' (Gravelines, France) and raised in the facilities of SEBIO (Le Havre, France) in 100 L tanks with aerated artificial seawater (18ºC temperature and 30‰ salinity - Tetra marine sea salt, Melle, Germany) under a photoperiod of 14 h light:10 h darkness. Physicochemical parameters (temperature, salinity, oxygen, ammonium, nitrate and nitrite) were assessed weekly before 80% of water renewal, as they were found to be stable and in optimal conditions according to the values recommended by Person-Le Ruyet *et al.* (1995). The animals were fed daily *ad libidum* with 'Turbot label rouge' fish feed (Le Gouessant, Lamballe, France). All fish were handled in accordance with the European Union regulations concerning the protection of experimental animals (Dir 2010/63/EU). At 452 days post-hatch (dph), 15 fish were randomly chosen and sacrificed with an overdose at 100 $mg \cdot L^{-1}$ MS-222 (Sigma-Aldrich, Saint-Louis, U.S.A.). Body weight and length were recorded, and the Fulton's condition factor (K) was calculated according to Hadidi *et al*. (2008). Gender was identified by macroscopic observation and confirmed post-hoc by gonad histology using hematoxylin-eosin-saffron staining. Males represented more than 90% of the sampled population, nevertheless all individuals were used for the experiment, since the sampling (April 2019) occurred outside the sea bass reproductive season. Whole thymus, spleen, liver and gonads were dissected. Spleen, liver and gonads were weighted and hepato-somatic (HSI), gonado-somatic (GSI) and spleno-somatic (SSI) indices were calculated according to Hadidi *et al*. (2008), Robinson *et al*. (2008) and Zha *et al*. (2007), respectively. Biometric indices of the fish used for the *in vitro* experiment are listed in Table S1.

2.2. Culture conditions and EE2-exposure

The thymus was gently passed through a 100 μm cell strainer adding Leibovitz medium (L15, Sigma). Thymocyte-enriched cell suspensions were obtained as described in Paiola *et al*. (2021) and the total number of thymocytes as well as their mortality was assessed by flow cytometry, after incubation of the cells with propidium iodide (PI) at 50 $\mu g \cdot mL^{-1}$ for 10 min in the darkness. Thymocytes were counted in 25 µL cell suspensions using a gating that selected all IP-negative thymocytes and thus excluded debris and dead cells. The proportion of T and B cells amongst all thymocytes was assessed by immunostaining using a *D. labrax* (DL) pan-T cell (DLT15+) and B cell (DLIg3+) specific monoclonal antibody, respectively (Scapigliati et al., 1995; Scapigliati et al., 2003). All flow cytometric measurements were carried out with a NovoCytes™ (ACEA Biosciences Inc., San Diego, USA) and analysed by NovoExpress® software (ACEA Biosciences Inc.). The results of flow cytometry are presented in Table S1. When needed, cell suspensions isolated from two individual fish of similar biometric indices were pooled in order to reach 2.5 x 10^6 $cells \cdot mL^{-1}$. Eventually, this resulted in six biological replicates for the solvent controls (n=6) and five for the cells treated with EE2 (n=5). Cells were incubated in L15 without phenol red for two hours in 25 cm^2 flasks at 17℃ to allow adhesion to occur. Subsequently, cells were exposed for four hours to 30 nM (*i.e.*, ~10 $ng \cdot L^{-1}$) EE2 (Sigma-Aldrich) diluted in 0.00001% (v/v) ethanol, or to the solvent control, *i.e*., L15 without phenol red and the equivalent concentration of ethanol. The concentration used in this study was a thousandfold lower than the reported EC_{20}-value for leukocyte cytotoxicity and about hundredfold less than the lowest observed effect concentration (LOEC) for selected immune parameters, such as phagocytosis or respiratory burst activity, for head kidney leucocytes from rainbow trout (*Oncorhynchus mykiss*) reported by Rehberger *et al*. (2021). After exposure, the medium was removed with a pipette and centrifuged at 4000 *g* for 10 min at 4°C to remove any non-adhering cells and debris and to collect the extracellular proteome present in the supernatant. Finally, samples were frozen at -80°C until further processing.

2.3. Proteomics

2.3.1. Sample preparation for quantitative label free analysis

Collected supernatants of either solvent control or EE2-treated cells were lyophilized. Two technical replicates for each sample, *i.e*., biological replicate, were resuspended and pooled in a total volume of 500 µL of ammonium bicarbonate buffer (100 mM) and then submitted to

centrifugation at 4000 *g* for 20 min at 4°C. Each supernatant was submitted to diafiltration by 10 volumes of ammonium bicarbonate (100 mM) on Amicon ultra 3K filters (Merck Millipore, Molsheim, France) and concentrated to obtain a final volume of 50 µL.

Collected supernatants were mixed with 5X Laemmli Buffer (0.312 M Tris-HCL, pH 6.8, 50% w/v Glycerol, 10% w/v SDS, 0.25% Bromophenol blue) and heated for 10 min at 100°C. Samples were then loaded on a 7% bis-acrylamide gel. Electrophoresis was performed for approximately 3 h at 10°C using fixed amperage of 20 mA in a Tris-Glycine buffer (14% Glycine, 3% Tris base, 2% SDS). Gels were briefly stained (30 sec) under shaking in Coomassie blue R-250 solution (30% ethanol, 10% acetic acid, 0.02% Coomassie R-250) and destained for 30 min. Subsequently, protein bands of interest just above the migration front were cut out.

Excised protein bands were denatured in 5 mM Tris(2-CarboxyEthyl)Phosphine hydrochloride (TCEP, Sigma) combined with 100 mM ammonium bicarbonate buffer for 1 h at 56°C. Reduced cysteine residues were then blocked by incubation in 55 mM iodoacetamide (Sigma) for 20 min at room temperature in the dark, before performing in-gel trypsin digestion according to the manufacturer's instructions (Promega, Madison, U.S.A.). Trypsin-digested peptides were extracted twice through subsequent treatments with 1% formic acid/94% acetonitrile/5% formic acid (v/v) before being evaporated using a vacuum concentrator.

2.3.2. NanoLC-ESI-MS/MS analysis

Before running the nanoLC-ESI-MS/MS analysis, all peptide samples were resuspended in 10 µL of 5% acetonitrile/0.1% formic acid buffer/94.9 % H_2O (v/v). Two µL of each sample were then analysed on a Q-Exactive Plus Mass Spectrometer equipment (Thermo Scientific, Waltham, U.S.A.) equipped with a nanoESI source. Peptides were loaded onto an enrichment column (C18 Pepmap100, 5 mm x 300 µm, granulometry of 5 µm, porosity of 100 Å; Thermo Scientific) and separated on an EASY-spray column (50 cm x 75 µm, granulometry of 3 µm, porosity of 100 Å, Thermo Scientific) with a flow rate of 300 $\mu L \cdot min^{-1}$. The mobile phase was composed of H_2O/0.1% formic acid (buffer A) and acetonitrile/H_2O/0.1% formic acid (80/20) (buffer B). The elution gradient duration was 120 min following different steps: 0–84 min, 2–35% B; 84–94 min, 35–90% B; 94–105 min, 90% B; 106–120 min, 2% B. The temperature of the column was set at 40°C. The mass spectrometer acquisition parameters were: 100 ms maximum injection time, 1.6 kV capillary voltage, 275°C capillary temperature, full scan MS *m/z* @ 400–1800 with a resolution of 70,000 in MS and 17,500 in MS/MS. The 10 most intense ions ('Top 10') were selected and fragmented with nitrogen as a collision gas (normalized collision energy set to 27 eV). For subsequent data analysis (2.3.3.) the spectra were exported in ".raw" format.

2.3.3. Quantitative label free proteomic data Analysis

In order to identify the proteins regulated between control *versus* EE2-treated cells, the Progenesis LC-MS software (Nonlinear dynamics, version 4.1) was used for protein alignment. Automatic alignment was set to perform two by two comparisons between samples in order to align the LC-MS runs and consider any retention time drifts. A minimum of 80% alignment score was required for further analysis. After alignment, statistical analysis was performed with Mann-Whitney U-test, as the data did not follow normal distribution and homoscedasticity. To highlight peptides differentially displayed between solvent control and EE2-treatment, the α-level was set at 5% ($p \leq 0.05$). The peak list containing the differentially expressed peptides was then used for identification by Mascot (Matrix Science, version 2.5, Boston, MA) with the following parameters: enzyme specificity, trypsin; one missed cleavage permitted; variable modifications, carbamidomethylation (C); oxidation (M), pyro-glu from E and Q; monoisotopic precursor mass tolerance: 5 ppm; product mass tolerance: 0.02 Da against the seabass genome database (http://seabass.mpipz.mpg.de/DOWNLOADS, Tine et al., 2014). A positive match was considered when it was ranked among the first positions and presented a score with a significant threshold of $p \leq 0.05$ and a false discovery rate (FDR) below 1. Mascot search results were imported back into Progenesis for identification of differentially regulated protein with at least two peptides.

2.3.4. Bioinformatics Analyses

Gene ontology (GO) term and pathway (KEGG) enrichment analyses were carried out using ClueGO (v2.5.5) and Cytoscape (v3.7.0), comparing the list of 111 differentially displayed consisting of 21 upregulated and 90 downregulated proteins (see results section) against the *Danio rerio* (zebrafish) set of GO biological process and molecular function databases (using July 2021 updates). Prior to this, *D. rerio* proteins corresponding to the 111 sea bass proteins were obtained using stand-alone BlastX against the Ensembl zebrafish protein predictions (downloaded from https://www. ensembl.org in October 2019), with E value < 10^{-10}.

The following settings were used for the ClueGO enrichment analysis (right-side): GO levels 3 to 8, Benjamini-Hochberg FDR correction with a cut-off at FDR < 0.05 and minimum of three genes/4% for terms to be considered significant. The initial group size was set as 1, group merging at 50% and Kappa-statistics score at 0.4. Enrichment scores of the functionally related network groups were calculated as -Log_2[group FDR]. The leading terms of each enriched group were those with the lowest term FDR (highest enrichment score) and were used to name the respective group.

Hierarchical clustering of the 111 differentially displayed proteins was performed using the Cluster 3.0 sofware (available from http://bonsai.hgc.jp/~mdehoon/software/cluster/ software.htm#ctv) using normalized protein (area) levels, with uncentered correlation and complete linkage options to produce heatmaps of protein levels, visualized by Java TreeView 1.1.6r4.

In silico identification of potentially secreted proteins among the 111 differentially displayed proteins was carried out using four different 'software pipelines', based on previous studies (Emanuelsson et al., 2007; Gogleva et al., 2018 and Caccia et al., 2013). Three pipelines focused on the classical secretion pathway: Pipeline 1 ran PHOBIUS (Käll et al., 2004) + TargetP (Emanuelsson et al., 2000) predictions; Pipeline 2 ran SignalP 5.0 (Armenteros et al., 2019) + TMHMM 2.0 (Sonnhammer et al., 1998) and Pipeline 3 ran SignalP 5.0 (Armenteros et al., 2019) + TMHMM 2.0 (Sonnhammer et al., 1998) + WOLFSORT (Horton et al., 2007). And another pipeline focused on non-classical pathway predictions: SecretomeP 2.0 (Bendtsen et al., 2005). Proteins containing a signal peptide supported by at least three of the four pipelines were classified as potentially secreted *via* the classical pathway. In case these proteins contained a transmembrane helix (as predicted by the TMHMM) or were located in an intracellular compartment (as predicted by WOLFSORT), they were removed from the list of the proteins predicted to be secreted by the classical pathway. Proteins with a SecretomeP score exceeding 0.5 were classified as potentially secreted by the non-classical pathway. It should be noted, that proteins with an accumulated peptide length of less than 40 amino acids could not be analysed by the above-mentioned programmes (*i.e.*, 'not analysable' in Tab. 1 and 2).

3. Results

3.1. Extracellular proteome changes in response to EE2 exposure

The thymocyte-enriched cell suspensions consisted of ~83% DLT15+ cells (T cells), ~16.6% progenitor T cells and ~0.4% DLIg3+ cells (B Cells). Mortality rates of individual cell suspensions tested prior to exposure were found to be less than 1.5 %. Protein abundances were quantified in each of the 11 individual extracellular protein profiles, *i.e.*, six biological replicates from solvent control (C1- C6) and five from EE2-treated cells (EE1- EE5). Of these (n=111), only 34% proteins corresponded to protein predictions of low confidence, *i.e.*, containing the designations '-like', '-probable' or '–uncharacterised'.

Among the proteins identified against the sea bass genome, statistical analysis identified differentially displayed proteins at $p \leq 0.05$ and with an FDR < 0.01 (Table S2). From these, 21 proteins, summarised in Table 1, presented increased levels in the EE2-treated group ranging between 1.24 and 0.42 Log_2-fold change. Table 2 displays the summarized identification and quantification details from the 90 proteins that were significantly downregulated at an FDR < 0.01

in suspensions from EE2-treated cells. Downregulations ranged from -5.19 to -0.42 Log_2-fold change. Detailed quantification, identification and secretion prediction results for the identified 111 differentially displayed proteins can be consulted in Table S2.

3.2. Hierarchical clustering of differentially produced proteins

The proteins that were differentially displayed between control and EE2-treated cells were clustered in a heatmap to visualise the patterns of up- and downregulation clearly distinguishing EE2-treated cells from control cells (Fig. 1).

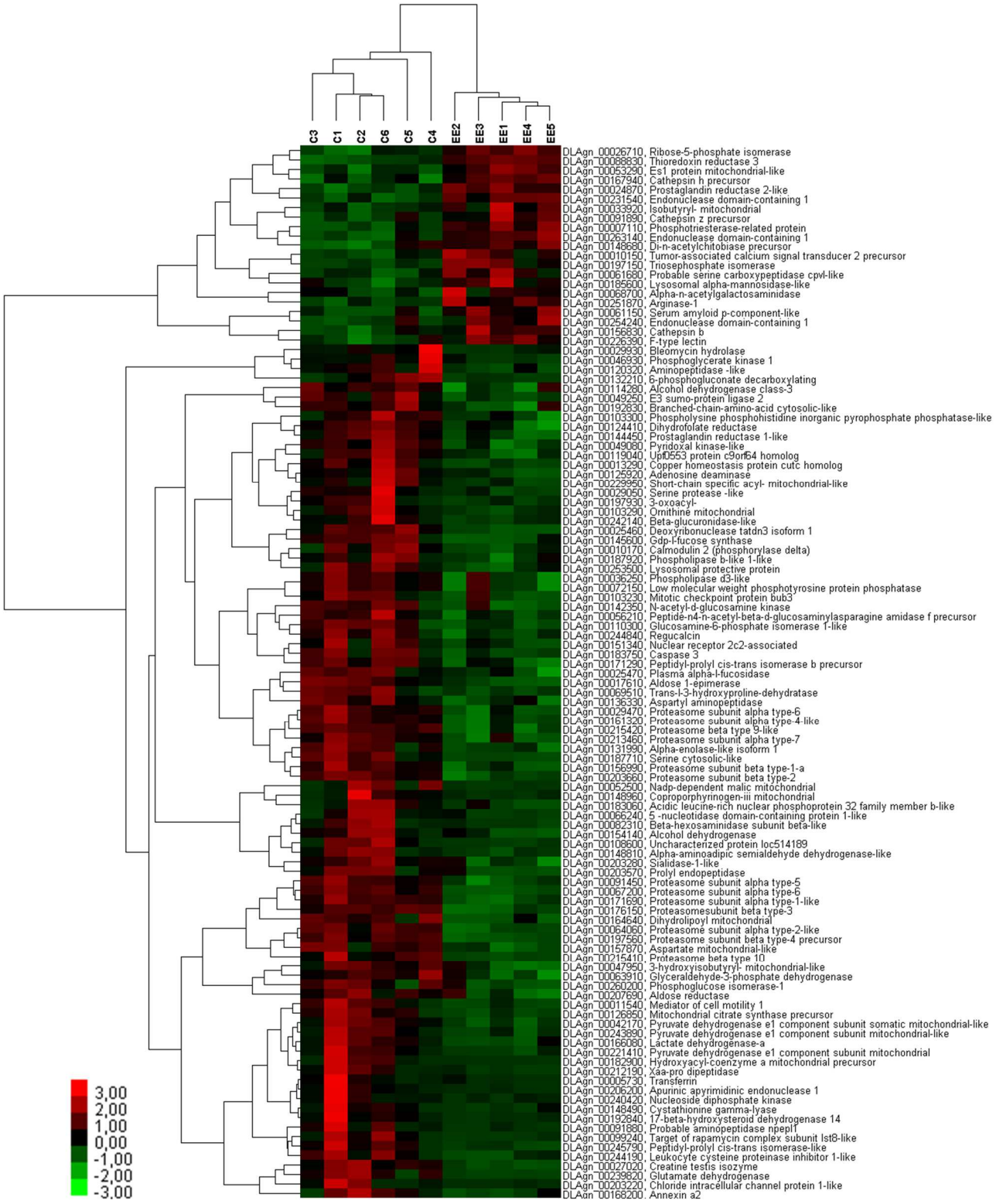

Fig. 1. Hierarchical clustering of differentially displayed proteins. The heat map clusters the 111 proteins with significantly different Log_2-fold changes between control and EE2-treated thymocytes. Each column represents the profile of one biological replicate; controls (C), 6 columns on the left-hand side; EE2-treated (EE) cells, 5 columns on the right. Colour scale: -3 to 3 Log_2-fold (from light green to red).

Table 1. Increased Log_2-fold changes (FC) of significantly upregulated proteins (FDR < 0.01 and p-value < 0.05 [Mann-Whitney]) between EE2-treated and control cell suspensions. Sec = secretion classification, based on *in silico* predictions (for details see 2.3.4. Bioinformatics Analyses); CP = Classical Pathway, ? = equivocal status, - = not analysable.

Accession	Description	Avg C	Avg EE2	p-value	LOG2(FC)	Sec
DLAgn_00263140	Endonuclease domain-containing 1	1.34E+05	3.17E+05	0.004	1.24	CP
DLAgn_00251870	Arginase-1	3.93E+04	8.57E+04	0.004	1.13	?
DLAgn_00010150	Tumor-associated calcium signal transducer 2 precursor/ epithelial cell adhesion molecule	7.74E+05	1.57E+06	0.017	1.02	-
DLAgn_00061150	Serum amyloid p-component-like	2.15E+05	4.10E+05	0.017	0.93	CP
DLAgn_00231540	Endonuclease domain-containing 1	8.59E+04	1.58E+05	0.004	0.88	?
DLAgn_00254240	Endonuclease domain-containing 1	5.71E+05	1.04E+06	0.030	0.87	CP
DLAgn_00197150	Triosephosphate isomerase	4.08E+05	7.41E+05	0.004	0.86	-
DLAgn_00026710	Ribose-5-phosphate isomerase	1.37E+07	2.31E+07	0.004	0.75	-
DLAgn_00091890	Cathepsin z precursor	4.12E+06	6.94E+06	0.017	0.75	CP
DLAgn_00226390	F-type lectin	5.80E+04	9.75E+04	0.017	0.75	CP
DLAgn_00024870	Prostaglandin reductase 2-like	2.47E+05	4.02E+05	0.004	0.70	?
DLAgn_00088830	Thioredoxin reductase 3	1.83E+05	2.91E+05	0.004	0.67	-
DLAgn_00156830	Cathepsin b	2.53E+06	4.02E+06	0.009	0.67	CP
DLAgn_00053290	Es1 protein mitochondrial-like	3.52E+07	5.49E+07	0.004	0.64	-
DLAgn_00007110	Phosphotriesterase-related protein	7.78E+06	1.19E+07	0.004	0.61	-
DLAgn_00061680	Probable serine carboxypeptidase cpvl-like	2.57E+06	3.91E+06	0.030	0.61	CP
DLAgn_00185600	Lysosomal alpha-mannosidase-like	1.44E+06	2.18E+06	0.009	0.59	CP
DLAgn_00167940	Cathepsin h precursor	1.86E+06	2.77E+06	0.004	0.58	CP
DLAgn_00033920	Isobutyryl- mitochondrial	6.45E+05	9.61E+05	0.017	0.57	CP
DLAgn_00148680	Di-n-acetylchitobiase precursor	1.53E+05	2.11E+05	0.035	0.46	CP
DLAgn_00068700	Alpha-n-acetylgalactosaminidase	8.52E+04	1.14E+05	0.0303	0.42	CP

Table 2. Log_2fold change (FC) of significantly downregulated proteins (FDR < 0.01 and p-value < 0.05 [Mann-Whitney]) between EE2-exposed and control cell suspensions. Sec = secretion classification, based on *in silico* predictions (for details see 2.3.4. Bioinformatics Analyses); CP = Classical Pathway, NCP = Non-Classical Pathway, ? = equivocal status, - = not analysable.

Accession	Description	Avg C	Avg EE2	p-value	LOG2(FC)	Sec
DLAgn_00239820	Glutamate dehydrogenase	9.72E+03	2.67E+02	0.017	-5.19	?
DLAgn_00203220	Chloride intracellular channel protein 1-like	1.89E+04	9.54E+02	0.017	-4.31	-
DLAgn_00182900	Hydroxyacyl-coenzyme a mitochondrial precursor	1.05E+05	5.78E+03	0.009	-4.19	-
DLAgn_00052500	Nadp-dependent malic mitochondrial	6.23E+04	3.82E+03	0.030	-4.03	-
DLAgn_00027020	Creatine testis isozyme	7.95E+03	5.53E+02	0.004	-3.85	-
DLAgn_00099240	Target of rapamycin complex subunit lst8-like	2.97E+04	2.16E+03	0.009	-3.78	?
DLAgn_00187710	Serine cytosolic-like	1.18E+04	8.78E+02	0.004	-3.74	-
DLAgn_00192840	17-beta-hydroxysteroid dehydrogenase 14	2.06E+04	1.85E+03	0.004	-3.48	-
DLAgn_00132210	6-phosphogluconate decarboxylating	2.79E+04	2.58E+03	0.017	-3.44	-
DLAgn_00206200	Apurinic apyrimidinic endonuclease 1	4.42E+05	4.23E+04	0.004	-3.38	NCP

DLAgn_00091880	Probable aminopeptidase npepl1	4.93E+04	4.80E+03	0.009	-3.36	-
DLAgn_00005730	Transferrin	1.01E+04	1.20E+03	0.017	-3.08	CP
DLAgn_00108600	Uncharacterized protein loc514189	1.29E+05	1.58E+04	0.004	-3.03	-
DLAgn_00212190	Xaa-pro dipeptidase	9.26E+03	1.21E+03	0.017	-2.94	-
DLAgn_00197930	3-oxoacyl-[acyl-carrier-protein] synthase	8.71E+03	1.14E+03	0.030	-2.93	-
DLAgn_00066240	5 -nucleotidase domain-containing protein 1-like	1.80E+05	2.48E+04	0.030	-2.86	-
DLAgn_00245790	Peptidyl-prolyl cis-trans isomerase-like	5.70E+06	8.25E+05	0.017	-2.79	-
DLAgn_00029930	Bleomycin hydrolase	4.58E+04	7.06E+03	0.017	-2.70	-
DLAgn_00011540	Mediator of cell motility 1	5.77E+04	9.35E+03	0.009	-2.62	?
DLAgn_00240420	Nucleoside diphosphate kinase	8.45E+04	1.39E+04	0.004	-2.60	?
DLAgn_00215410	Proteasome beta type 10	2.64E+03	4.48E+02	0.004	-2.56	-
DLAgn_00013290	Copper homeostasis protein cutc homolog	1.17E+04	2.01E+03	0.004	-2.54	?
DLAgn_00148960	Coproporphyrinogen-iii mitochondrial	2.88E+04	5.03E+03	0.017	-2.52	-
DLAgn_00164640	Dihydrolipoyl mitochondrial	3.46E+05	6.27E+04	0.009	-2.46	-
DLAgn_00069510	Trans-l-3-hydroxyproline-dehydratase	1.74E+04	3.31E+03	0.030	-2.40	-
DLAgn_00082310	Beta-hexosaminidase subunit beta-like	1.64E+06	3.15E+05	0.017	-2.38	CP
DLAgn_00126850	Mitochondrial citrate synthase precursor	1.66E+06	3.23E+05	0.009	-2.36	-
DLAgn_00203570	Prolyl endopeptidase	4.05E+04	7.97E+03	0.030	-2.34	?
DLAgn_00017610	Aldose 1-epimerase	7.93E+04	1.65E+04	0.004	-2.27	-
DLAgn_00197560	Proteasome subunit beta type-4 precursor	6.29E+04	1.35E+04	0.004	-2.23	-
DLAgn_00145600	Gdp-l-fucose synthase	4.74E+04	1.02E+04	0.009	-2.22	-
DLAgn_00049250	E3 sumo-protein ligase 2	8.95E+03	1.94E+03	0.004	-2.20	-
DLAgn_00151340	Nuclear receptor 2c2-associated	3.09E+04	6.75E+03	0.030	-2.20	?
DLAgn_00064060	Proteasome subunit alpha type-2-like	1.03E+05	2.24E+04	0.004	-2.19	?
DLAgn_00029050	Serine protease -like	6.57E+04	1.47E+04	0.009	-2.16	CP
DLAgn_00120320	Aminopeptidase -like	1.01E+06	2.30E+05	0.017	-2.14	-
DLAgn_00103290	Ornithine mitochondrial	2.54E+05	5.79E+04	0.009	-2.13	-
DLAgn_00148810	Alpha-aminoadipic semialdehyde dehydrogenase-like	3.34E+05	7.65E+04	0.009	-2.13	?
DLAgn_00148490	Cystathionine gamma-lyase	1.03E+05	2.36E+04	0.030	-2.13	-
DLAgn_00183750	Caspase 3	8.63E+04	2.01E+04	0.017	-2.10	-
DLAgn_00221410	Pyruvate dehydrogenase e1 component subunit mitochondrial	6.27E+04	1.47E+04	0.009	-2.09	?
DLAgn_00010170	Calmodulin 2 (phosphorylase delta)	3.27E+04	7.71E+03	0.017	-2.09	?
DLAgn_00260200	Phosphoglucose isomerase-1	1.08E+06	2.56E+05	0.030	-2.07	-
DLAgn_00067200	Proteasome subunit alpha type-6	4.87E+04	1.19E+04	0.004	-2.03	-
DLAgn_00166080	Lactate dehydrogenase-a	1.78E+04	4.64E+03	0.017	-1.94	?
DLAgn_00215420	Proteasome beta type 9-like	8.08E+03	2.31E+03	0.004	-1.81	-
DLAgn_00103230	Mitotic checkpoint protein bub3	1.04E+04	3.05E+03	0.030	-1.78	-
DLAgn_00183060	Acidic leucine-rich nuclear phosphoprotein 32 family member b-like	7.79E+05	2.32E+05	0.030	-1.75	?
DLAgn_00244190	Leukocyte cysteine proteinase inhibitor 1-like	5.95E+04	1.82E+04	0.017	-1.71	-
DLAgn_00046930	Phosphoglycerate kinase 1	3.19E+05	9.86E+04	0.030	-1.69	-
DLAgn_00042170	Pyruvate dehydrogenase e1 component subunit somatic mitochondrial-like	1.76E+05	5.49E+04	0.004	-1.68	-
DLAgn_00203660	Proteasome subunit beta type-2	2.29E+04	7.43E+03	0.004	-1.62	-
DLAgn_00110300	Glucosamine-6-phosphate isomerase 1-like	2.77E+05	9.40E+04	0.030	-1.56	-

DLAgn_00243890	Pyruvate dehydrogenase e1 component subunit mitochondrial-like	2.20E+05	7.54E+04	0.011	-1.55	-
DLAgn_00168200	Annexin a2	9.12E+04	3.17E+04	0.030	-1.53	-
DLAgn_00176150	Proteasome subunit beta type-3	1.07E+05	3.87E+04	0.004	-1.46	-
DLAgn_00131990	Alpha-enolase-like isoform 1	4.43E+04	1.61E+04	0.011	-1.46	-
DLAgn_00229950	Short-chain specific acyl- mitochondrial-like	3.11E+05	1.14E+05	0.009	-1.45	-
DLAgn_00025460	Deoxyribonuclease tatdn3 isoform 1	2.71E+04	1.04E+04	0.004	-1.38	-
DLAgn_00136330	Aspartyl aminopeptidase	1.18E+07	4.67E+06	0.030	-1.34	-
DLAgn_00161320	Proteasome subunit alpha type-4-like	7.36E+04	2.91E+04	0.004	-1.34	-
DLAgn_00125920	Adenosine deaminase	2.58E+07	1.03E+07	0.004	-1.32	-
DLAgn_00144450	Prostaglandin reductase 1-like	3.15E+06	1.30E+06	0.009	-1.27	-
DLAgn_00244840	Regucalcin	2.19E+04	9.44E+03	0.017	-1.22	-
DLAgn_00047950	3-hydroxyisobutyryl- mitochondrial-like	3.94E+05	1.76E+05	0.017	-1.16	-
DLAgn_00124410	Dihydrofolate reductase	6.71E+05	3.03E+05	0.004	-1.15	-
DLAgn_00154140	Alcohol dehydrogenase	2.51E+05	1.16E+05	0.030	-1.12	-
DLAgn_00142350	N-acetyl-d-glucosamine kinase	3.87E+05	1.79E+05	0.017	-1.12	?
DLAgn_00049080	Pyridoxal kinase-like	5.59E+05	2.65E+05	0.004	-1.08	-
DLAgn_00213460	Proteasome subunit alpha type-7	7.99E+04	3.89E+04	0.030	-1.04	-
DLAgn_00171690	Proteasome subunit alpha type-1-like	1.73E+05	8.51E+04	0.004	-1.03	?
DLAgn_00171290	Peptidyl-prolyl cis-trans isomerase b precursor	1.74E+07	8.60E+06	0.017	-1.02	-
DLAgn_00157870	Aspartate mitochondrial-like	3.12E+05	1.57E+05	0.009	-0.99	-
DLAgn_00253500	Lysosomal protective protein	2.69E+05	1.39E+05	0.017	-0.96	?
DLAgn_00187920	Phospholipase b-like 1-like	1.76E+05	9.14E+04	0.030	-0.95	CP
DLAgn_00025470	Plasma alpha-l-fucosidase	2.90E+05	1.52E+05	0.028	-0.93	CP
DLAgn_00091450	Proteasome subunit alpha type-5	2.19E+05	1.15E+05	0.004	-0.92	-
DLAgn_00119040	Upf0553 protein c9orf64 homolog	5.25E+05	2.84E+05	0.009	-0.89	-
DLAgn_00156990	Proteasome subunit beta type-1-a	1.44E+05	7.86E+04	0.004	-0.87	-
DLAgn_00207690	Aldose reductase	1.88E+05	1.03E+05	0.030	-0.87	-
DLAgn_00029470	Proteasome subunit alpha type-6	1.05E+05	5.91E+04	0.004	-0.83	-
DLAgn_00056210	Peptide-n4-n-acetyl-beta-d-glucosaminylasparagine amidase f precursor	2.09E+05	1.20E+05	0.009	-0.79	CP
DLAgn_00192830	Branched-chain-amino-acid cytosolic-like	2.80E+05	1.64E+05	0.017	-0.77	-
DLAgn_00242140	Beta-glucuronidase-like	1.46E+06	8.65E+05	0.009	-0.75	-
DLAgn_00036250	Phospholipase d3-like	4.40E+05	2.72E+05	0.046	-0.69	-
DLAgn_00072150	Low molecular weight phosphotyrosine protein phosphatase	4.40E+05	2.72E+05	0.046	-0.69	?
DLAgn_00114280	Alcohol dehydrogenase class-3	5.29E+06	3.37E+06	0.030	-0.65	-
DLAgn_00203280	Sialidase-1-like	5.82E+05	3.75E+05	0.017	-0.63	CP
DLAgn_00063910	Glyceraldehyde-3-phosphate dehydrogenase	9.44E+07	6.12E+07	0.017	-0.62	-
DLAgn_00103300	Phospholysine phosphohistidine inorganic pyrophosphate phosphatase-like	1.06E+06	7.39E+05	0.009	-0.52	-

3.3. Association of proteins to GO functional categories and biological pathways

Enrichment analysis was carried out using the selected dataset consisting of the 111 differentially displayed proteins, as well as for the sub-lists comprising the 21 upregulated and the 90 downregulated proteins (Tab. S2). Based on the zebrafish protein functional annotations, several GO terms could be assigned to the proteins, integrating them into either of the GO functional categories ‘Biological Process’ (BP) or ‘Molecular Function’ (MF), as well as several KEGG

pathways. Within each classification, the significantly enriched terms (FDR < 0.05; see lists in Tables S3-S8) were assembled into groups of functionally related terms by Cytoscape/ClueGO analysis sorted by the highest enrichment score.

The list of the 21 upregulated proteins did not yield any significantly enriched GO term or KEGG pathways, probably due to the low number of proteins. The global enrichment analysis of all 111 differentially displayed proteins (as summarized in Fig. S1) gave in general very similar results to the analysis of the 90 downregulated proteins, which accounted for most of the changes in protein levels reported in this study (Fig. 2). The ClueGO network view of all significantly enriched GO biological processes or KEGG pathway terms, which are organized in groups and their respective interactions, is depicted in Fig. 3.

In the GO Biological Process category, 52 GO terms were significantly enriched among the downregulated proteins (Table S6), which were grouped into 8 groups of functional related GO terms; the groups with the highest enrichment scores belonged to 'Carboxylic acid metabolic process' (enrichment score 72.0) and 'Oxoacid metabolic process' (62.9). Interestingly, these two main groups of biological processes were strongly interconnected, as shown in Fig. 3A and B.

In the Molecular Function category, 19 GO terms were grouped into 9 functional related GO terms (Table S7). Furthermore, the enrichment analysis uncovered 17 significant KEGG biological pathways (listed in Table S8), which were grouped into 8 main (representative) KEGG categories. the pathway with the highest enrichment score belonged to 'Proteasome' (45.2), which was followed by a large group of 10 interconnected enriched KEGG pathways that were designated after its most significant pathway, *i.e.*, 'Glycolysis/Gluconeogenesis' with an enrichment score of 38.3 (Fig. 2, Fig. 3C and D as well as Table S8).

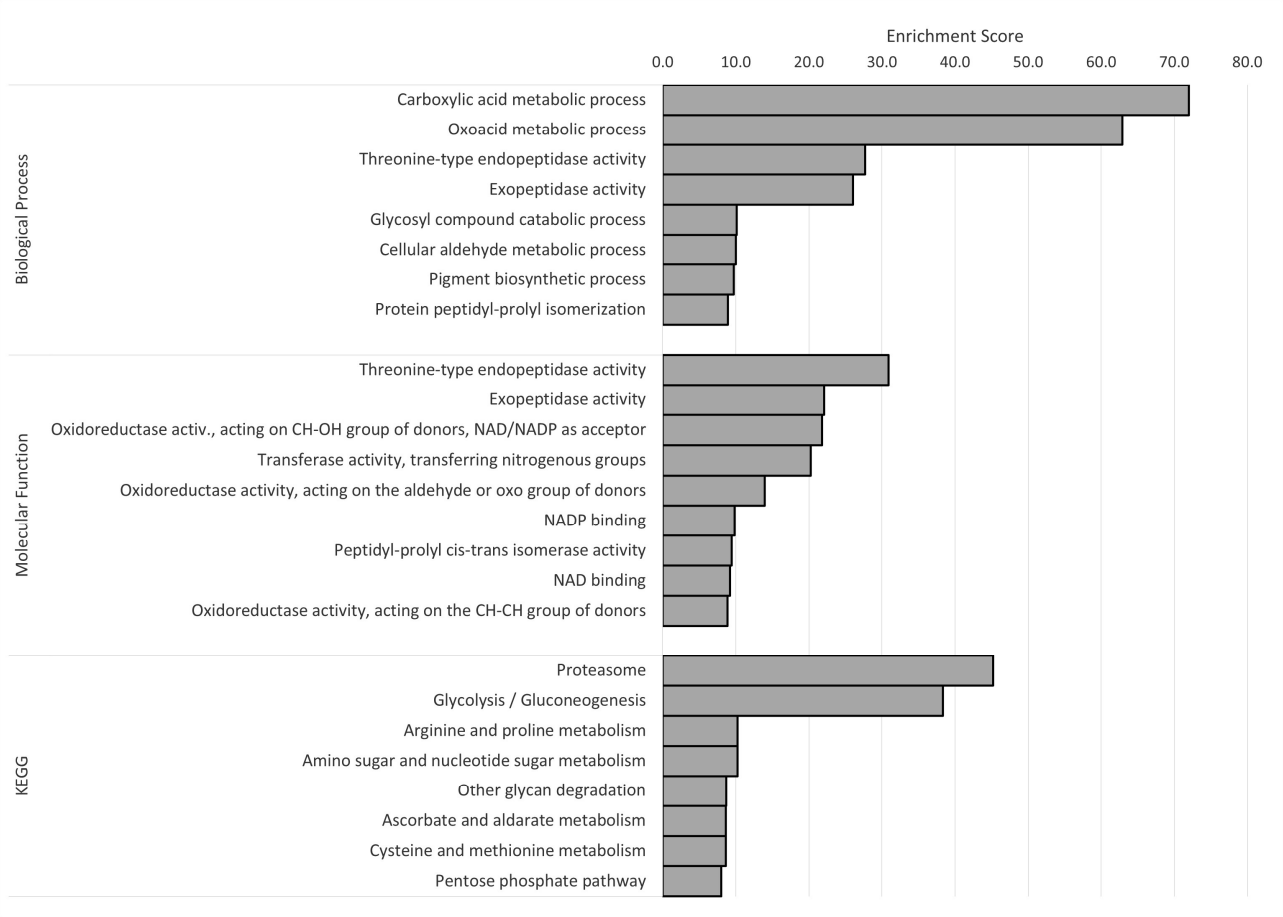

Fig. 2. Functional enrichment analyses showing the main Biological Processes, Molecular Functions and KEGG Pathways comprising the 90 proteins downregulated between control and EE2-treated thymocytes. Enrichment for gene ontology (GO) terms was carried out using the ClueGO plugin and Cytoscape software with the minimum significance set at 0.05 FDR. Represented groups had a significant enrichment (FDR <

0.05) and associated related significant GO terms according to their functional classification. Each group is labelled after its most significant term. Bar length corresponds to the significance of each group in the ClueGO network output measured by enrichment score ($-\log_2$ (group FDR)). For detailed lists of significantly enriched GO terms and groups consult Tables S6-S8.

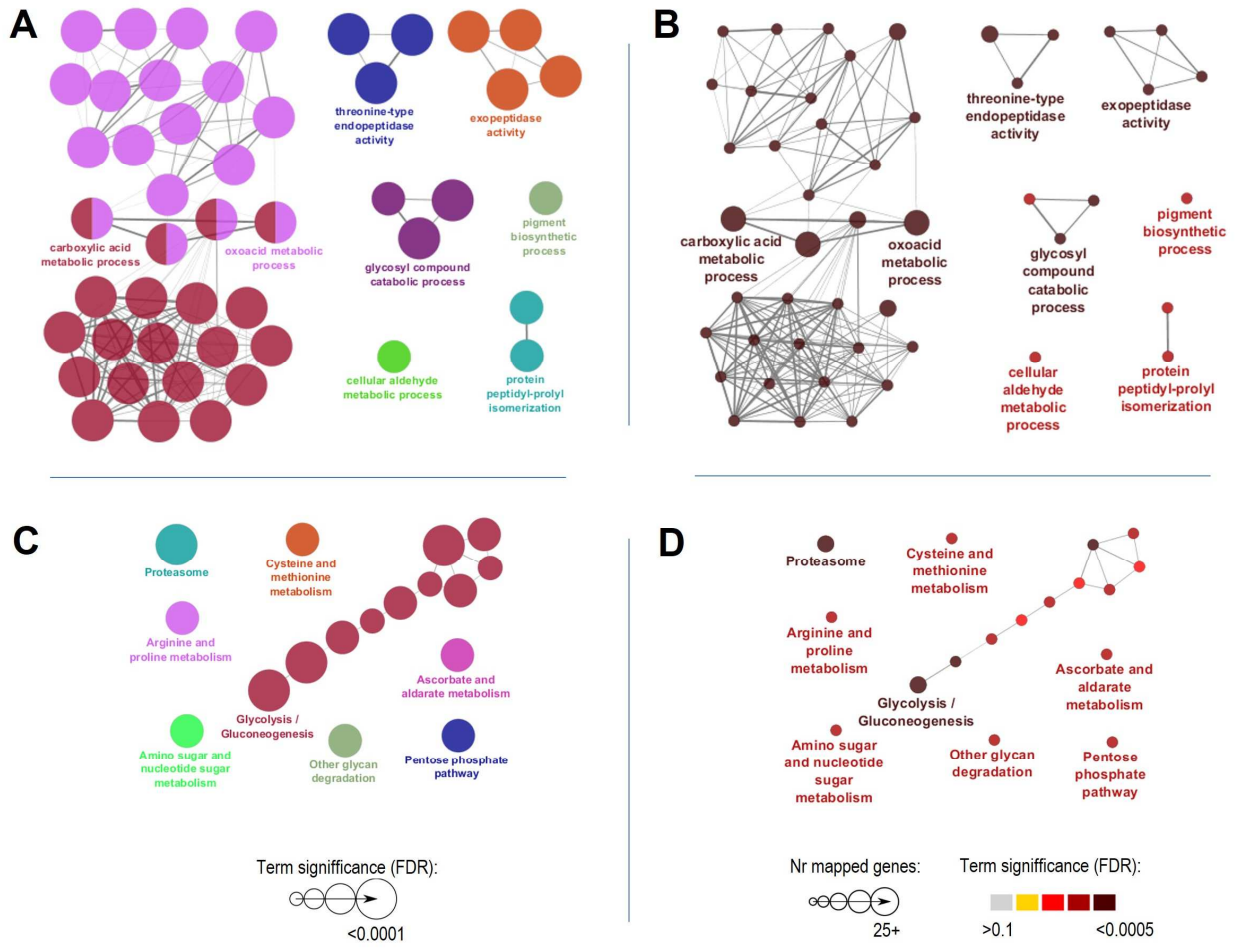

Fig. 3. Network view of the Gene ontology (GO) term (A-B) and pathway (KEGG) enrichment analyses (C-D) significantly enriched among the 90 proteins downregulated between control and EE2-treated thymocytes. Nodes (depicted as circles) represent each significantly enriched GO biological process/KEGG pathway (FDR<0.05), coloured according to their functional groups in A and C, or to the term significance in C and D (following the supplied colour legend). In addition, circle sizes represent the term significances (A and C) or number of mapped genes (B and D) – see legends at the bottom. Detailed enrichment results can be found in Tables S6 and S8; enrichment scores per group are summarized in Fig. 2. Biological processes/pathway terms or groups connected with lines are functionally associated according to the ClueGO/CluePedia analysis (for details see 2.3.4. Bioinformatics Analyses).

3.4. Potentially secreted proteins

Among the 111 differentially regulated proteins, 20 proteins were identified as potentially secreted by the classical or non-classical pathway. From these, 12 proteins were upregulated and 8 proteins were downregulated, in the samples treated with EE2, as compared to the control samples. The identification of the potentially secreted proteins can be found in Table 1 and Table 2. An overview of the 'pipeline' results is presented in Table S2.

4. Discussion

The secretome comprises a collection of peptides and proteins that are secreted by the cells and serve cell-to-cell communication (Mukherjee and Mani, 2013). The secretome may account for 10 to 20 % of the entire proteome (Zullo et al., 2015). Typical secretory proteins and peptides are

hormones, cytokines and chemokines, which regulate, among others, proliferation, growth and nutrition as well as digestive enzymes, such as proteases. The classical pathway of secretion requires that these peptides have a signal peptide. This characteristic of secreted proteins can be used to identify them in the secretome. In addition, unconventional protein secretion has been acknowledged. Protein secretion involving non-classical pathways uses membranous organelles of different size and origin, such as exosomes and microvesicles, to release proteins into the extracellular environment (Nickel, 2005; Mathivanan et al., 2010; Zullo et al., 2015). In this case, the signal peptide is absent. Inevitably, the origin of such proteins must remain ambiguous as, theoretically, dying cells could release their protein content into the culture medium by apoptotic budding (Mukherjee and Mani, 2013; Zullo et al., 2015). Provided that cell viability was high, it is questionable, whether cell death could have fundamentally influenced the secretomes of EE2-stimulated and non-stimulated thymocytes. Mortality in the present study was always lower than 1.5% (Tab. S1), so that contamination by intracellular proteins from dying cells was considered insignificant. It is, therefore, unlikely that any minor cell death that may have occurred in both the control and EE2-treated cells would be responsible for the observed differential display, notably the downregulation of extracellular proteasome and upregulation of cathepsins in EE2-stimulated cells. Accordingly, although oestrogen can alter thymocyte viability *in vitro*, this was observed in sea bass thymocytes only after 48 h of exposure; no significant effects on thymocyte viability were detectable at 2 and 24 h of oestrogen-exposure (Paiola et al. 2019).

The GO term and KEGG enrichment analysis yielded significant results for the 90 downregulated proteins only, because the number of upregulated proteins was insufficient as to obtain reliable pathway information. It should be noted, however, that upregulation of proteins in thymocyte enriched cell-suspensions was putatively related to secretion, as more than 50% of the upregulated proteins were predicted to be secreted by the classical pathway, *i.e.*, to present precursors featuring a signal peptide. Hence, it appears that EE2-exposure stimulates the secretory activity of thymocytes. In the following, we will concentrate on those proteins, which were represented more than once among the proteins that were either down- or upregulated, respectively.

Amongst the proteins downregulated by EE2-stimulation, enrichment analysis indicated the proteasome to be one of the most impacted pathways (KEGG pathways, Fig. S1 and Fig. 2). Earlier secretome analyses from human and murine samples have revealed proteasome subunits to be part of the extracellular proteins secreted by the non-classical pathway (Alvarez-Llamas et al., 2007; Chevallet et al., 2007; Sixt and Dahlmann, 2008). Bochman *et al*. (2014) demonstrated that human T lymphocytes actively export proteasomes through microvesicles into the extracellular environment, so that the passive efflux of proteasomes from dead cells could be excluded. Furthermore, these authors conclude that the proteasome subunits must be released from the microvesicles as circulating proteasomes can be quantified by ELISA assays. They show that free proteasomes can be released from microvesicles by sphingolipid hydrolysing enzymes, thus providing some evidence for a proteasome releasing mechanism by which proteolytically active 20S and subunits of the 19S proteasome regulator could be ‘secreted’ into the extracellular environment (Bochman et al., 2014). However, the role of extracellular proteasomes must not be proteolysis. They could also act as paracrine factors or as regulators of cell proliferation (Sixt and Dahlmann, 2008; Bochmann et al., 2014). Maturing thymocytes undergo extensive proliferation, but at the same time selection results in apoptosis of more than 90% of the developing thymocytes (Takahama, 2006). Dieudé *et al*. (2015) demonstrated that apoptotic cells release exosomes containing proteolytically active proteasome. Such paracrine apoptotic processes could also play a role in the selection of thymocytes within the thymus. In this case, EE2 would downregulate selection associated apoptosis, which should result in a less efficient selection process leading to thymic hypertrophy as observed in mice by Forsberg (1996) and sea bass by Seemann *et al*. (2015). However, oestradiol-treatment was mostly found to induce thymus atrophy in mice as a result of increased apoptosis thus eliminating ETPs and by decreasing proliferation (Novotny et al., 1983, Mor et al., 2001, Okasha et al., 2001; Zoller and Kersh, 2006). The downregulation of proteasomes

would, therefore, rather be coherent with their role of regulators of cell proliferation. It remains, however, unclear how this role would be integrated into a paracrine signalling-cascade between thymocytes and the TECs.

That EE2-exposure of thymocytes *in vitro* primarily affects T cell proliferation rather than apoptosis is further supported by the downregulation of caspase-3 (Tab. 2), as thymocyte apoptosis in mice was found to be associated with high levels of cleaved caspase-3 (Albu et al., 2007). Our results confirm those of earlier studies, in Wall lizard, *Hemidactylus flaviviridis*, and sea bass: Hareramadas and Rai (2006) found no evidence for apoptosis when they exposed thymocytes *in vitro* to E2 in the range of 10^{-15} to 10^{-5}M, but a clear inhibition of the proliferation of concanavalin A induced mitogenic thymocytes; Paiola *et al*. (2018), did not observe any modulation of the initiator caspases-8 and -9 that activate caspase-3 through cleavage in *D. labrax* injected with E2 at 0.5 $mg \cdot kg^{-1}$. Interestingly, glycolysis drives caspase-3 activation in mice (Secinaro et al., 2018), but the complex glycolysis/gluconeogenesis appeared to be downregulated in the present study (Fig. 2 and 3), further supporting the hypothesis that EE2 affected T cell proliferation rather than T cell apoptosis.

Decreased proliferation would also be coherent with the upregulation of arginase 1 (Tab. 1) and the downregulation target of rapamycin complex 1 (TORC1; Tab. 2) found in this study. Arginase 1 is known to deplete arginine in the microenvironment, thereby limiting nutrient availability for developing thymocytes and suppressing T cell proliferation (Munder et al., 2006; Czystowska-Kuzmicz et al., 2019). In mice, arginine deprivation was followed by declining TORC1 activity (Van de Velde et al., 2017). Indeed, TORC1 provides a link between nutrients that fuel the high energy demand of proliferating thymocytes. TORC1, therefore, functions as a key regulator of T cell differentiation (Howden et al., 2019). The inhibition of TORC1 was found to impair cell cycle progression in activated naïve thymocytes in mice, putatively by reducing energy supply, *i.e.*, glucose and amino acids (Howden et al., 2019). This is confirmed by enrichment analyses in the present study, which showed a downregulation of carboxylic acid and cellular amino acid metabolic process, glucose 6-phosphate metabolism (Fig. 2 and 3, Tab. S6) as well as KEGG-pathways of glycolysis, amino sugar and amino acid metabolism and pentose phosphate pathway (Fig. 2 and 3, Tab. S8). Several mitochondrial proteins also displayed reduced levels in the extracellular proteome (Tab. 2), suggesting a reduction as described by Howden *et al*. (2019) following TORC1-inhibition. Hence, EE2-treatment of thymocytes is likely to lead to a reduction in TORC1 and, as matter of consequence, reduced proliferation of developing thymocytes related to reduced energy metabolism. Interestingly, this confirms recent findings of Paiola *et al*. (2021), who found that thymus plasticity and function in *D. labrax* is driven by the energetic trade-offs between thymocyte number and, putatively, ontogeny, and gonad development, the latter being communicated to the thymus *via* sex steroid hormones. It is likely, that the EE2-treatment induces signals from the thymocytes that lead to a remodelling of the thymic environment *via* the TECs and/or extracellular matrix (see below), as TORC1-inhibition also affects cell adhesion molecules in mice (Howden et al., 2019; Liang et al., 2019).

Although no specific pathway was upregulated in the secretome of EE2-stimulated thymocytes, three cathepsins—or their precursors—were increasingly secreted following EE2-treatment (Tab. 1). Cathepsins are versatile lysosomal proteases of which about 15 different classes exist (Patel et al., 2018). Cathepsins can also be found in the extracellular environment (Vizovisek et al., 2019; Vidak et al., 2019). Notably, cathepsin-E, expressed by immune cells, is a key regulator in major histocompatibility complex class II antigen presentation (Honey et al., 2002; Zaidi and Kalbacher, 2008; Stoeckle et al., 2012). The cathepsins-L and -V are also expressed in the thymus (Patel et al., 2018; Vidak et al., 2019). Interestingly, cathepsins may stimulate cell-to-cell communication, as it was found that cathepsin inhibitors negatively affected RANKL-signalling in mice (Kang et al., 2017). Cathepsins may exert a similar role in the thymus as haemopoietic cells, such as mouse DN4+ thymocytes, express RANKL to establish a proper thymic microenvironment and self-tolerance (Rossi et al., 2007; Hikosaka et al., 2008; Akiyama et al., 2008). Increase in cathepsins

may, therefore, inhibit RANK-signalling between developing thymocytes and TECs, thus reducing the medullar thymic environment. In this context, their extracellular role may also be seen in extracellular matrix remodelling of the thymic microenvironment (Lombardi et al., 2005; Vizovisek et al., 2019). Moreover, in cathepsin-L deficient mice, positive selection is impaired and CD4+ cells are significantly reduced (Lombardi et al., 2005). At the same time the thymic output of CD8+ cells increased. These authors suggest that cathepsin acts on the extracellular matrix components present in the thymus that promote the proliferation of thymocytes *via* integrin-signalling. The effects of cathepsins on the extracellular matrix could, therefore, affect the crosstalk between developing thymocytes and the thymic epithelial environment by lowering the paracrine signalling through hormones, chemokines and growth factors as well as thymocyte integrin-TEC ligand interactions. Notably, Lombardi *et al*. (2005) provide evidence that this complex is likely to have favoured the shift from CD4+ to CD8+ and conclude that cathepsin-L deficiency apparently affects lineage commitment. On the contrary, it is difficult to infer from these results of cathepsin-deficiency on cathepsin-overexpression. It may be speculated that EE2-treament induces cathepsins and that these are secreted or released through microvesicles from thymocytes. Subsequently, the upregulation of extracellular cathepsins could negatively affect thymic architecture and, in turn, reduce the TEC-promoted proliferation of thymocytes and unbalance lineage commitment. Furthermore, cathepsins apparently have role in regulation of T cell migration, as shown *in vitro* by Staun-Ram and Miller (2011), as cathepsin-S and -B specific inhibitors reduced T cell migration. They also demonstrated that interferon-β reduced cathepsin-S and T cell migration and they observed and increase of cathepsin-S secretion of monocytes in the presence of interferon-γ. The letter suggests that signalling proteins may provoke a non-canonical secretion of cathepsins, which may provide a link to the cathepsins upregulated in the thymocyte secretome in the present study. Conversely, an increase in cathepsins would accelerate migration. Accordingly, EE2 would stimulate the migration of thymocytes. Eventually, extracellular cathepsins could also process other signalling pathways mediated by cytokines and chemokines, or act on surface receptors and cell adhesion molecules (see below) (Vidak et al., 2019), thus influencing the cellular crosstalk between thymocytes and TECs. For instance, TECs may use the proenzyme form of cathepsin-L as a cofactor to promote proliferation of double-negative CD4-8-thymocytes in the mouse-thymus under the influence of IL-1 and IL-7 (Kasai et al., 1993). Inversely, it is possible that thymocytes use cathepsin for cell communication as well.

As mentioned above, the structural basis of thymus function consists of a reticular network of diverse TECs. The epithelial cell adhesion molecule (EpCAM), also called Tumor-associated calcium signal inducer 1 (TACSTD-1), which was upregulated about two-fold in EE2-treated thymocytes (Tab. 1), is expressed by most epithelia and is involved in processes fundamental for morphogenesis, including cell-cell adhesion, proliferation, differentiation, and migration (Schnell et al., 2013). The molecular mechanisms inducing the formation of the highly connected, three-dimensional network-organisation of the thymic epithelium through which the thymocytes migrate and differentiate are still unknown. In the thymic medulla, a major site of tolerance induction, the development of the epithelial cell net is tightly regulated by the requirements of thymocyte selection. These reticulated epithelial cells express high levels of the EpCAM molecule. Guillemot *et al*. (2001) have utilised different mouse-derived thymic epithelial cell lines and found that transfection with EpCAM enhanced cell growth and lead to a rapid reorganization of the actin cytoskeleton by inducing the formation of numerous stress fibres and long cell protrusions. Their results suggest that expression of EpCAM might balance the organising capacity of cadherin molecules and may be participating in the formation of the thymic architecture. Short term exposure of thymocytes to EE2 may trigger the release of EpCAM in order to maintain a dynamic stromal cell network in the thymus as demonstrated by Guillemot *et al*. (2001). As soon as thymocyte development restarts, this allows for a revitalisation of thymocyte proliferation and differentiation without having to rebuilt the three-dimensional epithelial network.

5. Conclusion

Overall, although much of the interpretation remains speculative in nature, the results seem to confirm the theory that oestrogens provide a hormonal signal that halts the proliferation and maturation of thymocytes. Even if the number of differentially displayed proteins that were found to be present in the extracellular proteome was low as compared to cellular proteomes, the downregulation of metabolic pathways and biological functions is coherent with a reduced proliferation of thymocytes and conforms with the life history theory that describes the optimisation of fundamental biological functions as a trade-off between reproduction and immunity. For the thymus, this involves a halt of growth or a reduction in volume when priority is given to reproductive functions, such gonad development (Kernen et al., 2020; Paiola et al., 2021). Oestrogens then provide a signal that directly affects the thymocytes, which relay the changes in metabolic state and energy available for thymocyte development to the surrounding stromal cells, resulting in a changed thymic architecture and, eventually, thymus involution. Eventually, the oestrogenic modulation of the thymus provides a target for environmental oestrogens, such as EE2, to interfere with the immune function of fish, and, potentially, to result in immunosuppression.

Acknowledgements

This work was supported by the ANR financed project ETaT (ANR-15-CE32-0014), Rouen University, Inserm, Normandy Region and European Regional Development Fund (ERDF). C.M. received a doctoral grant from Le Havre University. P.P. received Portuguese national funds from FCT - Foundation for Science and Technology, through project UIDB/04326/2020, a researcher contract with the University of Algarve under Norma Transitoria, reference DL57/2016/CP1361/CT0015, and from the scientific exchange programme of Le Havre University through an invited researcher period. The authors wish to thank Prof. G. Scapigliati, Tuscia University, for kindly providing the DLT15+ and DLIg3+ antibodies.

Conflict of interest

The authors declare no conflict of interest.

5. References

Abramson, J., Anderson, G., 2017. Thymic Epithelial Cells. Annu. Rev. Immunol. 35, 85-118.

Albu, D. I., Feng, D., Bhattacharya, D., Jenkins, N. A., Copeland, N. G., Liu, P., Avram, D., 2007. BCL11B is required for positive selection and survival of double-positive thymocytes. J. Exp. Med. 204(12), 3003-3015.

Alvarez-Llamas, G., Szalowska, E., de Vries, M. P., Weening, D., Landman, K., Hoek, A., Wolffenbuttel, B. H., Roelofsen, H., Vonk, R. J., 2007. Characterization of the human visceral adipose tissue secretome. Mol. Cell Proteomics. 6(4), 589-600.

Akiyama, T., Shimo, Y., Yanai, H., Qin, J., Ohshima, D., Maruyama, Y., ... Inoue, J. I., 2008. The tumor necrosis factor family receptors RANK and CD40 cooperatively establish the thymic medullary microenvironment and self-tolerance. Immunity. 29(3), 423-437.

Anderson, G., Jenkinson, E. J., Rodewald, H. R., 2009. A roadmap for thymic epithelial cell development. Eur. J. Immunol. 39(7), 1694-1699.

Anderson, G., Takahama, Y., 2012. Thymic epithelial cells: working class heroes for T cell development and repertoire selection. Trends Immunol. 33(6), 256-263.

Armenteros, J. J. A., Tsirigos, K. D., Sønderby, C. K., Petersen, T. N., Winther, O., Brunak, S., ... Nielsen, H., 2019. SignalP 5.0 improves signal peptide predictions using deep neural networks. Nat. Biotechnol. 37(4), 420-423.

Bendtsen, J. D., Kiemer, L., Fausbøll, A., Brunak, S., 2005. Non-classical protein secretion in bacteria. BMC Microbiol. 5(1), 1-13.

Bodey, B., Siegel, S. E., Kaiser, H. E., 2004. Involution of the Mammalian Thymus and Its Role in the Overall Aging Process. In: Immunological Aspects of Neoplasia — The Role of the Thymus. Cancer Growth and Progression, vol 17. Springer, Dordrecht, pp. 147-165.

Boehm, T., Swann, J. B., 2013. Thymus involution and regeneration: two sides of the same coin?. Nat. Rev. Immunol. 13, 831-838.

Boehm, T., Swann, J. B., 2014. Origin and evolution of adaptive immunity. Annu. Rev. Anim. Biosci. 2(1), 259-283.

Bochmann, I., Ebstein, F., Lehmann, A., Wohlschlaeger, J., Sixt, S. U., Kloetzel, P. M., Dahlmann, B., 2014. T lymphocytes export proteasomes by way of microparticles: a possible mechanism for generation of extracellular proteasomes. J. Cell Mol. Med. 18(1), 59-68.

Boyd, R. L., Tucek, C. L., Godfrey, D. I., Izon, D. J., Wilson, T. J., Davidson, N. J., ... Hugo, P., 1993. The thymic microenvironment. Immunol. Today. 14(9), 445-459.

Caccia, D., Dugo, M., Callari, M., Bongarzone, I., 2013. Bioinformatics tools for secretome analysis. Biochim. Biophys. Acta, Proteins Proteomics. 1834(11), 2442-2453.

Chaudhry, M. S., Velardi, E., Dudakov, J. A., van den Brink, M. R., 2016. Thymus: the next (re) generation. Immunol. Rev. 271(1), 56-71.

Chevallet, M., Diemer, H., Van Dorssealer, A., Villiers, C., Rabilloud, T., 2007. Toward a better analysis of secreted proteins: the example of the myeloid cells secretome. Proteomics. 7(11), 1757-1770.

Cockburn, A., 1992. Evolutionary ecology of the immune system: Why does the thymus involute?. Funct. Ecol. 6, 364-370.

Czystowska-Kuzmincz, M., Sosnowska, A., Nowis, D., Ramji, K., Szajnik, M., Chlebowska-Tuz, J., et al., 2019. Small extracellular vesicles containing-1 suppress T cell responses and promote tumor growth in ovarian carcinoma. Nat. Communicat. 10:3000.

Dieudé, M., Bell, C., Turgeon, J., Beillevaire, D., Pomerleau, L., Yang, B., ... Hébert, M. J., 2015. The 20S proteasome core, active within apoptotic exosome-like vesicles, induces autoantibody production and accelerates rejection. Sci Transl. Med. 7(318), 318ra200.

Emanuelsson, O., Nielsen, H., Brunak, S., Von Heijne, G., 2000. Predicting subcellular localization of proteins based on their N-terminal amino acid sequence. J. Mol. Biol. 300(4), 1005-1016.

Emanuelsson, O., Brunak, S., Von Heijne, G., Nielsen, H., 2007. Locating proteins in the cell using TargetP, SignalP and related tools. Nat. Protoc. *2*(4), 953.

Farley, A. M., Morris, L. X., Vroegindeweij, E., Depreter, M. L., Vaidya, H., Stenhouse, F. H., ... Blackburn, C. C., 2013. Dynamics of thymus organogenesis and colonization in early human development. Dev.140(9), 2015-2026.

Forsberg, J. G., 1996. The different responses of the female mouse thymus to estrogen after treatment of neonatal, prepubertal, and adult animals. Cells Tissues Organs. 157(4), 275-290.

Froehlicher, M., Liedtke, A., Groh, K., López-Schier, H., Neuhauss, S. C., Segner, H., Eggen, R. I., 2009. Estrogen receptor subtype β2 is involved in neuromast development in zebrafish (*Danio rerio*) larvae. Dev. Biol. 330, 32-43.

Gameiro, J., Nagib, P., Verinaud, L., 2010. The thymus microenvironment in regulating thymocyte differentiation. Cell Adh. Migr. 4(3), 382-90.

Gould, K. A., Shull, J. D., Gorski, J., 2000. DES action in the thymus: inhibition of cell proliferation and genetic variation. Mol. Cell. Endocrinol. 170, 31-39.

Gogleva, A., Drost, H. G., Schornack, S., 2018. SecretSanta: flexible pipelines for functional secretome prediction. Bioinformatics. 34(13), 2295-2296.

Guillemot, J. C., Naspetti, M., Malergue, F., Montcourrier, P., Galland, F., Naquet, P., 2001. Ep-CAM transfection in thymic epithelial cell lines triggers the formation of dynamic actin-rich

protrusions involved in the organization of epithelial cell layers. Histochem. Cell Biol. 116(4), 371-378.

Hadidi, S., Glenney, G. W., Welch, T. J., Silverstein, J. T., Wiens, G. D., 2008. Spleen size predicts resistance of rainbow trout to *Flavobacterium psychrophilum* challenge. J. Immunol. 180(6), 4156-4165.

Haley, P. J., 2003. Species differences in the structure and function of the immune system. Toxicology. 188(1), 49-71.

Hareramadas, B., Rai, U., 2006. Cellular mechanism of estrogen-induced thymic involution in wall lizard: caspase-dependent action. J. Exp. Zool. 305A, 396–409.

Hince, M., Sakkal, S., Vlahos, K., Dudakov, J., Boyd, R., Chidgey, A., 2008. The role of sex steroids and gonadectomy in the control of thymic involution. Cell Immunol. 252, 122-138

Hikosaka, Y., Nitta, T., Ohigashi, I., Yano, K., Ishimaru, N., Hayashi, Y., ... Takahama, Y., 2008. The cytokine RANKL produced by positively selected thymocytes fosters medullary thymic epithelial cells that express autoimmune regulator. Immunity. 29(3), 438-450.

Holländer, G., Gill, J., Zuklys, S., Iwanami, N., Liu, C., Takahama, Y., 2006. Cellular and molecular events during early thymus development. Immunol. Rev. 209, 28-46.

Honey, K., Benlagha, K., Beers, C., Forbush, K., Teyton, L., Kleijmeer, M. J., ... Bendelac, A., 2002. Thymocyte expression of cathepsin L is essential for NKT cell development. Nat. Immunol. 3(11), 1069-1074.

Horton, P., Park, K. J., Obayashi, T., Fujita, N., Harada, H., Adams-Collier, C. J., Nakai, K., 2007. WoLF PSORT: protein localization predictor. Nucleic acids res. 35(suppl_2), W585-W587.

Howden, A., Hukelmann, J. L., Brenes, A., Spinelli, L., Sinclair, L. V., Lamond, A. I., Cantrell, D. A., 2019. Quantitative analysis of T cell proteomes and environmental sensors during T cell differentiation. Nat. Immunol. 20(11), 1542–1554.

Iwanowicz, L. R., Ottinger, C., 2009. Estrogens, estrogen receptors, and their role as immunoregulators in fish. In: G. Zaccone, J. Meseguer, A. Garcia-Ayala, B. Kapoor B (eds.). Fish defenses. Volume I. Immunology. Science Publishers, Enfield (NH), pp. 277-322.

Käll, L., Krogh, A., Sonnhammer, E. L., 2004. A combined transmembrane topology and signal peptide prediction method. J. Mol. Biol. 338(5), 1027-1036.

Kang, J. H., Jung, H., Yim, M., 2017. 3', 4', 7, 8-Tetrahydroxyflavone inhibits RANKL-induced osteoclast formation and bone resorption. Pharmazie. 72(3), 161-166.

Kasai, M., Shirasawa, T., Kitamura, M., Ishido, K., Kominami, E., Hirokawa, K., 1993. Proenzyme form of cathepsin L produced by thymic epithelial cells promotes proliferation of immature thymocytes in the presence of IL-1, IL-7, and anti-CD3 antibody. Cell Immunol. 150(1), 124-136.

Kernen, L., Rieder, J., Duus, A., Holbech, H., Segner, H., Bailey, C., 2020. Thymus development in the zebrafish (*Danio rerio*) from an ecoimmunology perspective. J. Exp. Zool. A Ecol. Integr. Physiol. 333A, 805-819.

Klein, L., Kyewski, B., Allen, P. M., Hogquist, K. A., 2014. Positive and negative selection of the T cell repertoire: what thymocytes see (and don't see). Nat. Rev. Immunol. 14(6), 377-391.

Klug, D. B., Carter, C., Gimenez-Conti, I. B., Richie, E. R., 2002. Cutting edge: thymocyte-independent and thymocyte-dependent phases of epithelial patterning in the fetal thymus. J. Immunol. 169(6), 2842-2845.

Lepletier, A., Chidgey, A. P., Savino, W., 2015. Perspectives for improvement of the thymic microenvironment through manipulation of thymic epithelial cells: a mini-review. Gerontology, 61(6), 504-514.

Liang, Z., Zhang, L., Su, H., Luan, R., Na, N., Sun, L., ... Zhao, Y., 2018. MTOR signaling is essential for the development of thymic epithelial cells and the induction of central immune tolerance. Autophagy. 14(3), 505-517.

Linker, R. A., Lee, D. H., Flach, A. C., Litke, T., van den Brandt, J., Reichardt, H. M., ... Lühder, F., 2015. Thymocyte-derived BDNF influences T-cell maturation at the DN3/DN4 transition stage. Eur. J. Immunol. 45(5):1326-38.

Litman, G. W., Rast, J. P., Fugmann, S. D., 2010. The origins of vertebrate adaptive immunity. Nat. Rev. Immunol. 10(8), 543-553.

Lombardi, G., Burzyn, D., Mundiñano, J., Berguer, P., Bekinschtein, P., Costa, H., ... Nepomnaschy, I., 2005. Cathepsin-L influences the expression of extracellular matrix in lymphoid organs and plays a role in the regulation of thymic output and of peripheral T cell number. J. Immunol. 174(11), 7022-7032.

Manley, N. R., Richie, E. R., Blackburn, C. C., Condie, B. G., Sage, J., 2011. Structure and function of the thymic microenvironment. Front. Biosci. (Landmark Ed). 16, 2461-2477.

Martín, A., Alonso, L. M., Gomez del Moral, M., Zapata, A. G., 1994. Morphometrical changes in the rat thymic lymphoid cells after treatment with two different doses of estradiol benzoate. Histol. Histopathol. 9(2), 281-286.

Mathivanan, S., Ji, H., Simpson, R. J., 2010. Exosomes: extracellular organelles important in intercellular communication. J. Proteomics. 73(10), 1907-1920.

Molloy, E. J., O'Neill, A. J., Grantham, J. J., Sheridan-Pereira, M., Fitzpatrick, J. M., Webb, D. W., Watson, R. W. G., 2003. Sex-specific alterations in neutrophil apoptosis: the role of estradiol and progesterone. Blood, 102(7), 2653-2659.

Mor, G., Muñoz, A., Redlinger, Jr. R., Silva, I., Song, J., Lim, C., Kohen, F., 2001. The role of the Fas/Fas ligand system in estrogen-induced thymic alteration. Am. J. Reproduct. Immunol. 46, 298-307.

Moreira, C., Paiola, M., Duflot, A., Varó, I., Sitjà-Bobadilla, A., Knigge, T., Pinto, P., Monsinjon, T., 2021. The influence of 17β-oestradiol on lymphopoiesis and immune system ontogenesis in juvenile sea bass, *Dicentrarchus labrax*. Dev. Comp. Immunol. 118, 104011.

Munder, M., Schneider, H., Luckner, C., Giese, T., Langhans, C.-D., Fuentes, J. M., Kropf, P., Mueller, I., Kolb, A., Modollel, M., Ho, A. D., 2006. Suppression of T cell functions by humans granulocyte arginase. Blood 108, 1627-1634.

Mukherjee, P., Mani, S., 2013. Methodologies to decipher the cell secretome. Biochim. Biophys. Acta, Protein Proteomics. 1834(11), 2226-2232.

Nakanishi, T., 1986. Seasonal changes in the humoral immune response and the lymphoid tissues of the marine teleost, *Sebastiscus marmoratus*. Vet. Immunol. Immunopathol. 12(1-4), 213-221.

Nickel, W., 2005. Unconventional secretory routes: direct protein export across the plasma membrane of mammalian cells. Traffic. 6, 607–614.

Novotny, E. A., Raveche, E. S., Sharrow, S., Ottinger, M., Steinberg, A. D., 1983. Analysis of thymocyte subpopulations following treatment with sex hormones. Clin. Immunol. Immunopathol. 28(2), 205-217.

Okasha, S. A., Ryu, S., Do, Y., McKallip, R. J., Nagarkatti, M., Nagarkatti, P. S., 2001. Evidence for estradiol-induced apoptosis and dysregulated T cell maturation in the thymus. Toxicology, 163(1), 49-62.

Patel, S., Homaei, A., El-Seedi, H. R., Akhtar, N., 2018. Cathepsins: Proteases that are vital for survival but can also be fatal. Biomed. Pharmacother., 105, 526-532.

Paiola, M., Knigge, T., Picchietti, S., Duflot, A., Guerra, L., Pinto, P. I., Scapigliati, G., Monsinjon, T., 2017. Oestrogen receptor distribution related to functional thymus anatomy of the European sea bass, *Dicentrarchus labrax*. Dev. Comp. Immunol. 77, 106-120.

Paiola, M., Knigge, T., Duflot, A., Pinto, P. I., Farcy, E., Monsinjon, T., 2018. Oestrogen, an evolutionary conserved regulator of T cell differentiation and immune tolerance in jawed vertebrates? Dev. Comp. Immunol. 84, 48-61.

Paiola, M., Moreira, C., Hétru, J., Duflot, A., Pinto, P. I., Scapigliati, G., Knigge, T., Monsinjon, T., 2021. Prepubertal gonad investment modulates thymus function: evidence in a teleost fish. J. Exp. Biol. 224, jeb238576.

Person-Le Ruyet, J., Chartois, H., Quemener, L., 1995. Comparative acute ammonia toxicity in marine fish and plasma ammonia response. Aquaculture 136 (1–2), 181-194.

Rehberger, K., Escher, B. I., Scheidegger, A., Werner, I., Segner, H., 2021. Evaluation of an in vitro assay to screen the immunotoxic potential of chemicals to fish. Sci. Rep. 11(1):3167

Ribeiro, A. R., Rodrigues, P. M., Meireles, C., Di Santo, J. P., Alves, N. L., 2013. Thymocyte selection regulates the homeostasis of IL-7–expressing thymic cortical epithelial cells in vivo. J. Immunol. 191(3), 1200-1209.

Rijhsinghani, A. G., Thompson, K., Bhatia, S. K., Waldschmidt, T. J., 1996. Estrogen blocks early T cell development in the thymus. Am. J. Reprod. Immunol. 36(5), 269-277.

Roberts, N. A., Desanti, G. E., Withers, D. R., Scott, H. R., Jenkinson, W. E., Lane, P. J., ... Anderson, G., 2009. Absence of thymus crosstalk in the fetus does not preclude hematopoietic induction of a functional thymus in the adult. Eur. J. Immunol. 39(9), 2395-2402.

Robinson, J., Aumeeruddy, R., Jörgensen, T. L., Öhman, M. C., 2008. Dynamics of camouflage (*Epinephelus polyphekadion*) and brown marbled grouper (*Epinephelus fuscoguttatus)* spawning aggregations at a remote reef site, Seychelles. Bull. Mar. Sci. 83(2), 415-431.

Rossi, S. W., Kim, M. Y., Leibbrandt, A., Parnell, S. M., Jenkinson, W. E., Glanville, S. H., ... Anderson, G., 2007. RANK signals from CD4+ 3− inducer cells regulate development of Aire-expressing epithelial cells in the thymic medulla. J. Exp. Med., 204(6), 1267-1272.

Scapigliati, G., Mazzini, M., Mastrolia, L., Romano, N., Abelli, L., 1995. Production and characterisation of a monoclonal antibody against the thymocytes of the sea bass *Dicentrarchus labrax* (L.) (Teleostea, Percicthydae). Fish Shellfish Immunol. 5, 393-405.

Scapigliati, G., Meloni, S., Buonocore, F., Bossu, P., Prugnoli, D., Secombes, C. J., 2003. Immunopurification of B lymphocytes from sea bass *Dicentrarchus labrax* (L.). J. Mar. Biotechnol. 5(3), 214-221.

Schnell, U., Cirulli, V., Giepmans, B. N. G., 2013. EpCAM: Structure and function in health and disease. Biochim. Biophys. Acta, Biomembr. 1828, 1989–2001.

Secinaro, M. A., Fortner, K. A., Dienz, O., Logan, A., Murphy, M. P., Anathy, V., Boyson, J. E., Budd, R. C., 2018. Glycolysis promotes caspase-3 activation in lipid rafts in T cells.

Segner, H., Casanova-Nakayama, A., Kase, R., Tyler, C. R., 2013. Impact of environmental estrogens on Yfish considering the diversity of estrogen signaling. Gen. Comp. Endocrinol. 191, 190-201.

Seiki, K., Sakabe, K., 1997. Sex hormones and the thymus in relation to thymocyte proliferation and maturation. Arch. Histol. Cytol. 60, 29-38.

Selvaraj, V., Bunick, D., Finnigan-Bunick, C., Johnson, R. W., Wang, H., Liu, L., Cooke, P. S., 2005. Gene expression profiling of 17β-estradiol and genistein effects on mouse thymus. Toxicol. Sci. 87(1), 97-112.

Seemann, F., Knigge, T., Olivier, S., Monsinjon, T., 2015. Exogenous 17 β-oestradiol (E2) modifies thymus growth and regionalization in European sea bass *Dicentrarchus labrax*. J. Fish Biol. 86(3), 1186-1198.

Shved, N., Berishvili, G., Baroiller, J. F., Segner, H., Reinecke, M., 2008. Environmentally relevant concentrations of 17α-ethinylestradiol (EE2) interfere with the growth hormone (GH)/insulin-like growth factor (IGF)-I system in developing bony fish. Toxicol. Sci. 106(1), 93-102.

Sixt, S. U., Dahlmann, B., 2008. Extracellular, circulating proteasomes and ubiquitin - incidence and relevance. Biochim. Biophys. Acta, Mol. Basis Dis. 1782(12), 817-823.

Sonnhammer, E. L., Von Heijne, G., Krogh, A., 1998. A hidden Markov model for predicting transmembrane helices in protein sequences. ISMB. 6, 175-182.

Staples, J. E., Gasiewicz, T. A., Fiore, N. C., Lubahn, D. B., Korach, K. S., Silverstone, A. E., 1999. Estrogen receptor α is necessary in thymic development and estradiol-induced thymic alterations. J. Immunol. 163(8), 4168-4174.

Staun-Ram, E., Miller, A., 2011. Cathepsins (S and B) and their inhibitor Cystatin C in immune cells: modulation by interferon-β and role played in cell migration. J. Neuroimmunol. 232(1-2), 200-206.

Straub, R. H., 2007. The complex role of estrogens in inflammation. Endocr. Rev. 28(5), 521-574.

Stoeckle, C., Quecke, P., Rückrich, T., Burster, T., Reich, M., Weber, E., Kalbacher, H., Driessen, C., Melms, A., Tolosa, E., 2012. Cathepsin S dominates autoantigen processing in human thymic dendritic cells. J. Autoimmun. 38(4), 332-343.

Szwejser, E., Maciuszek, M., Casanova-Nakayama, A., Segner, H., Verburg-van Kemenade, B. L., Chadzinska, M., 2017. A role for multiple estrogen receptors in immune regulation of common carp. Dev. Comp. Immunol. 66, 61-72.

Takahama, Y, 2006. Journey through the thymus: stromal guides for T cell development and selection. Nat. Rev. Immunol. 6(2), 127-135.

Tibbetts, T. A., DeMayo, F., Rich, S., Conneely, O. M., O'Malley, B. W., 1999. Progesterone receptors in the thymus are required for thymic involution during pregnancy and for normal fertility. Proc. Nat. Acad. Sci., 96(21), 12021-12026.

Tine, M., Kuhl, H., Gagnaire, P. A., Louro, B., Desmarais, E., Martins, R. S., ... & Reinhardt, R., 2014. European sea bass genome and its variation provide insights into adaptation to euryhalinity and speciation. Nat. Commun. 5(1), 1-10.

van Ewijk, W., Shores, E. W., Singer, A., 1994. Crosstalk in the mouse thymus. Immunol. Today. 15(5), 214-217.

Van de Velde, L.-A., Subramanian, C., Smith, A.M., Barron, L., Qualls, J.E., Neale, G., Alfonso-Pecchio, A., Jackowski, S., Rock, C. O., Wynn, T. A., Murray, P. J., 2017. T cells encountering myeloid cells programmes for amino acid-dependent nimmunosuppression use Rictor/mTORC2 protein for proliferation checkpoint decisions. J. Biol. Chem. 292, 15-30.

van Ewijk, W., Hollander, G., Terhorst, C., Wang, B., 2000. Stepwise development of thymic microenvironments in vivo is regulated by thymocyte subsets. Dev. 127(8), 1583-1591.

Vidak, E., Javoršek, U., Vizovišek, M., Turk, B., 2019. Cysteine cathepsins and their extracellular roles: shaping the microenvironment. Cells. 8(3), 264.

Vizovišek, M., Fonović, M., Turk, B., 2019. Cysteine cathepsins in extracellular matrix remodeling: Extracellular matrix degradation and beyond. Matrix Biol. 75, 141-159.

Wetie, A. G. N., Sokolowska, I., Woods, A. G., Wormwood, K. L., Dao, S., Patel, S., ... Darie, C. C., 2013. Automated mass spectrometry–based functional assay for the routine analysis of the secretome. J. Lab. Autom. 18(1), 19-29.

Yao, G., Hao, Y., 2004. Thymic atrophy *via* estrogen-induced apoptosis is related to Fas/FasL pathway. Int. Immunopharmacol. 4, 213–221.

Zoller, A. L., Kersh, G. J., 2006. Estrogen induces thymic atrophy by eliminating early thymic progenitors and inhibiting proliferation of β-selected thymocytes. J. Immunol. 176, 7371-7378.

Zaidi, N., Kalbacher, H., 2008. Cathepsin E: a mini review. Biochem. Biophys. Res. Commun. 367(3), 517-522.

Zha, J., Wang, Z., Wang, N., Ingersoll, C., 2007. Histological alternation and vitellogenin induction in adult rare minnow (*Gobiocypris rarus*) after exposure to ethynylestradiol and nonylphenol. Chemosphere. 66(3), 488-495.

Zullo, J., Matsumoto, K., Xavier, S., Ratliff, B., Goligorsky, M. S., 2015. The cell secretome, a mediator of cell-to-cell communication. Prostaglandins Other Lipid Mediat. 120, 17-20.

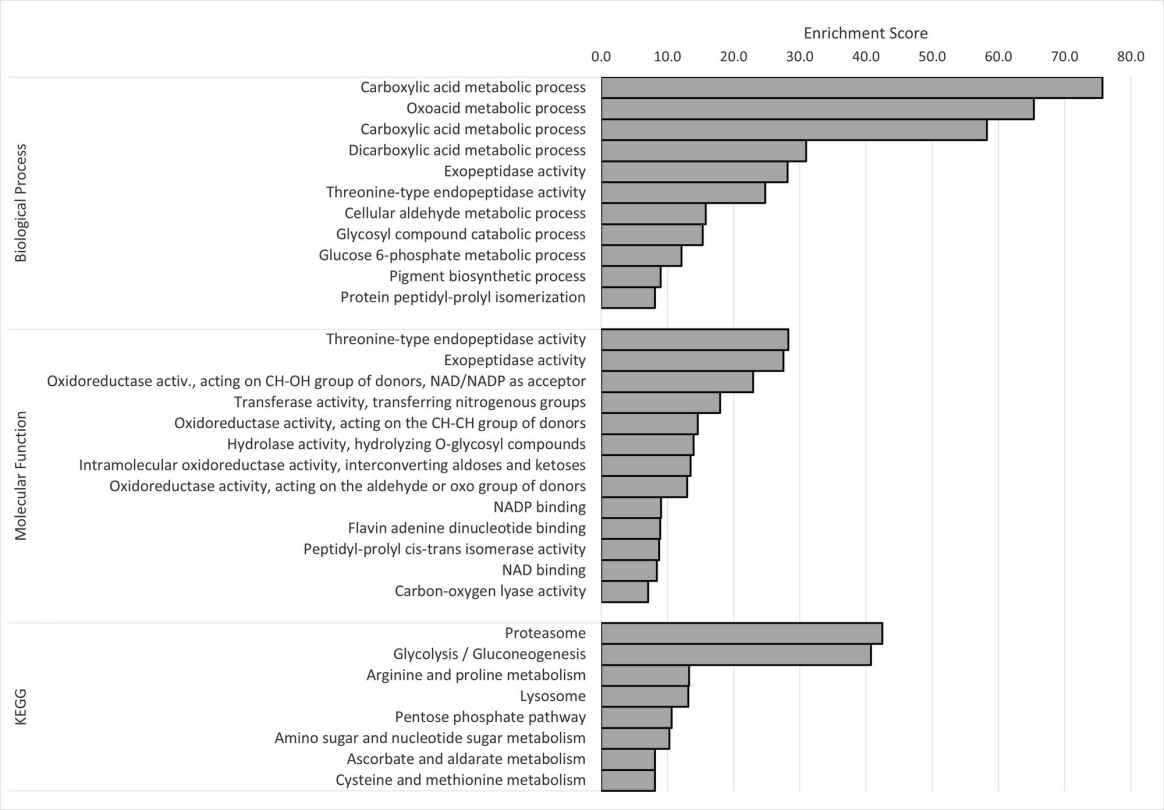
Enrichment Score
0.0
10.0
20.0
30.0
40.0
50.0
60.0
70.0
80.0
Biological Process
Carboxylic acid metabolic process
Oxoacid metabolic process
Carboxylic acid metabolic process
Dicarboxylic acid metabolic process
Exopeptidase activity
Threonine-type endopeptidase activity
Cellular aldehyde metabolic process
Glycosyl compound catabolic process
Glucose 6-phosphate metabolic process
Pigment biosynthetic process
Protein peptidyl-prolyl isomerization
Molecular Function
Threonine-type endopeptidase activity
Exopeptidase activity
Oxidoreductase activ., acting on CH-OH group of donors, NAD/NADP as acceptor
Transferase activity, transferring nitrogenous groups
Oxidoreductase activity, acting on the CH-CH group of donors
Hydrolase activity, hydrolyzing O-glycosyl compounds
Intramolecular oxidoreductase activity, interconverting aldoses and ketoses
Oxidoreductase activity, acting on the aldehyde or oxo group of donors
NADP binding
Flavin adenine dinucleotide binding
Peptidyl-prolyl cis-trans isomerase activity
NAD binding
Carbon-oxygen lyase activity
KEGG
Proteasome
Glycolysis / Gluconeogenesis
Arginine and proline metabolism
Lysosome
Pentose phosphate pathway
Amino sugar and nucleotide sugar metabolism
Ascorbate and aldarate metabolism
Cysteine and methionine metabolism

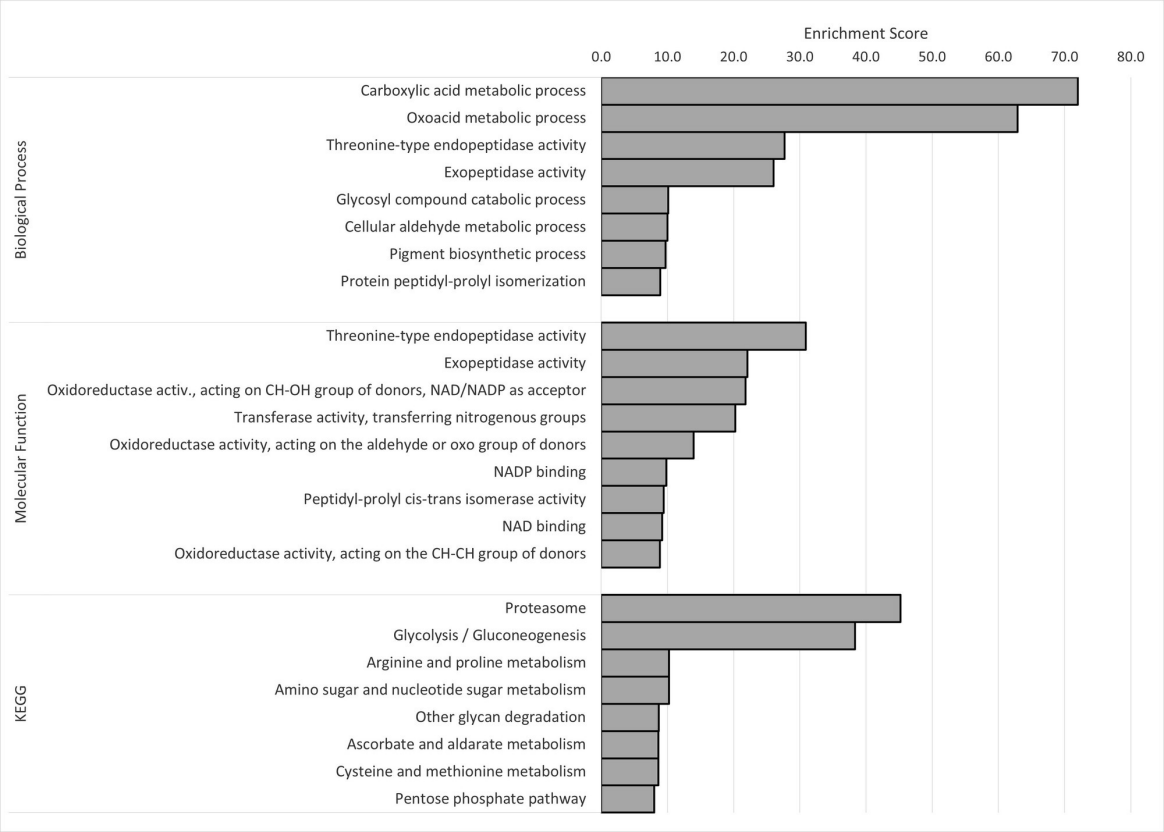
Enrichment Score
0.0
10.0
20.0
30.0
40.0
50.0
60.0
70.0
80.0
Biological Process
Carboxylic acid metabolic process
Oxoacid metabolic process
Threonine-type endopeptidase activity
Exopeptidase activity
Glycosyl compound catabolic process
Cellular aldehyde metabolic process
Pigment biosynthetic process
Protein peptidyl-prolyl isomerization
Molecular Function
Threonine-type endopeptidase activity
Exopeptidase activity
Oxidoreductase activ., acting on CH-OH group of donors, NAD/NADP as acceptor
Transferase activity, transferring nitrogenous groups
Oxidoreductase activity, acting on the aldehyde or oxo group of donors
NADP binding
Peptidyl-prolyl cis-trans isomerase activity
NAD binding
Oxidoreductase activity, acting on the CH-CH group of donors
KEGG
Proteasome
Glycolysis / Gluconeogenesis
Arginine and proline metabolism
Amino sugar and nucleotide sugar metabolism
Other glycan degradation
Ascorbate and aldarate metabolism
Cysteine and methionine metabolism
Pentose phosphate pathway

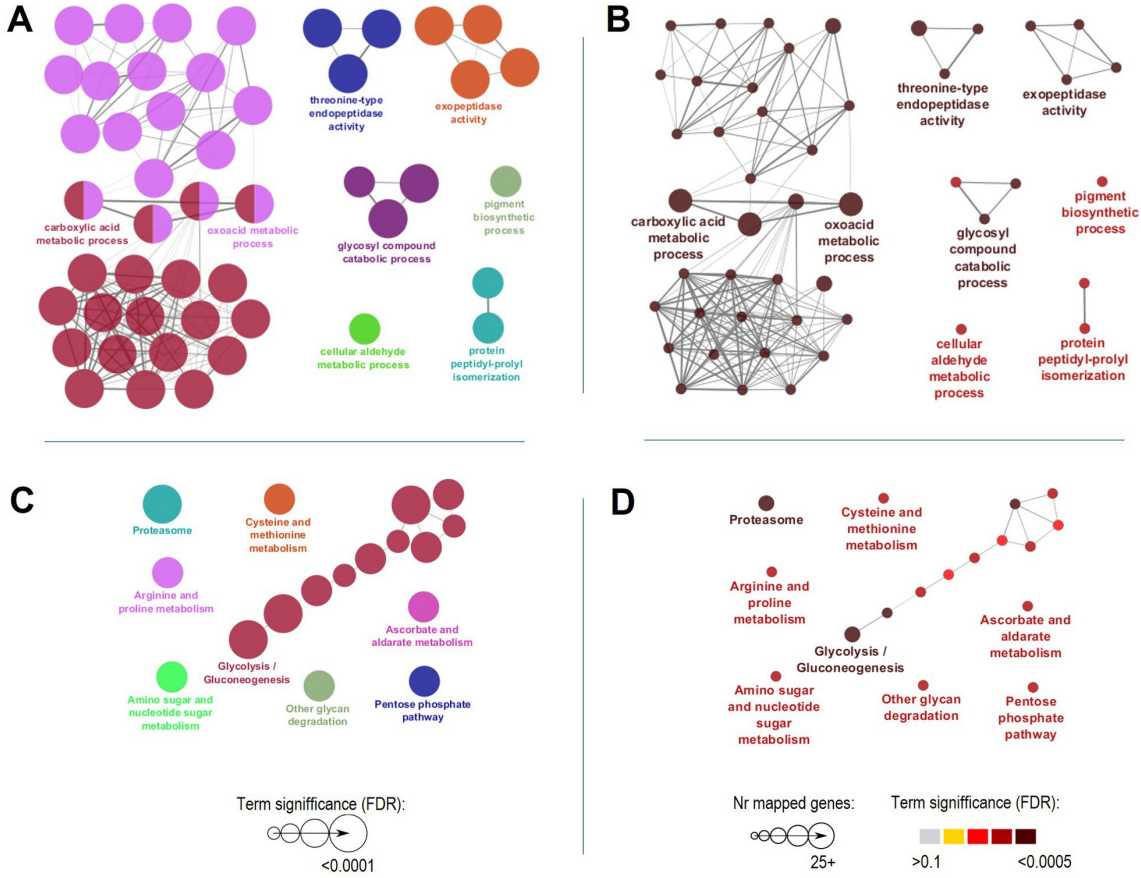
A
threonine-type endopeptidase activity
exopeptidase activity
carboxylic acid metabolic process
oxoacid metabolic process
glycosyl compound catabolic process
pigment biosynthetic process
cellular aldehyde metabolic process
protein peptidyl-prolyl isomerization
B
threonine-type endopeptidase activity
exopeptidase activity
carboxylic acid metabolic process
oxoacid metabolic process
glycosyl compound catabolic process
pigment biosynthetic process
cellular aldehyde metabolic process
protein peptidyl-prolyl isomerization
C
Proteasome
Cysteine and methionine metabolism
Arginine and proline metabolism
Ascorbate and aldarate metabolism
Glycolysis / Gluconeogenesis
Amino sugar and nucleotide sugar metabolism
Other glycan degradation
Pentose phosphate pathway
Term significance (FDR):
<0.0001
D
Proteasome
Cysteine and methionine metabolism
Arginine and proline metabolism
Ascorbate and aldarate metabolism
Glycolysis / Gluconeogenesis
Amino sugar and nucleotide sugar metabolism
Other glycan degradation
Pentose phosphate pathway
Nr mapped genes:
25+
Term significance (FDR):
>0.1
<0.0005

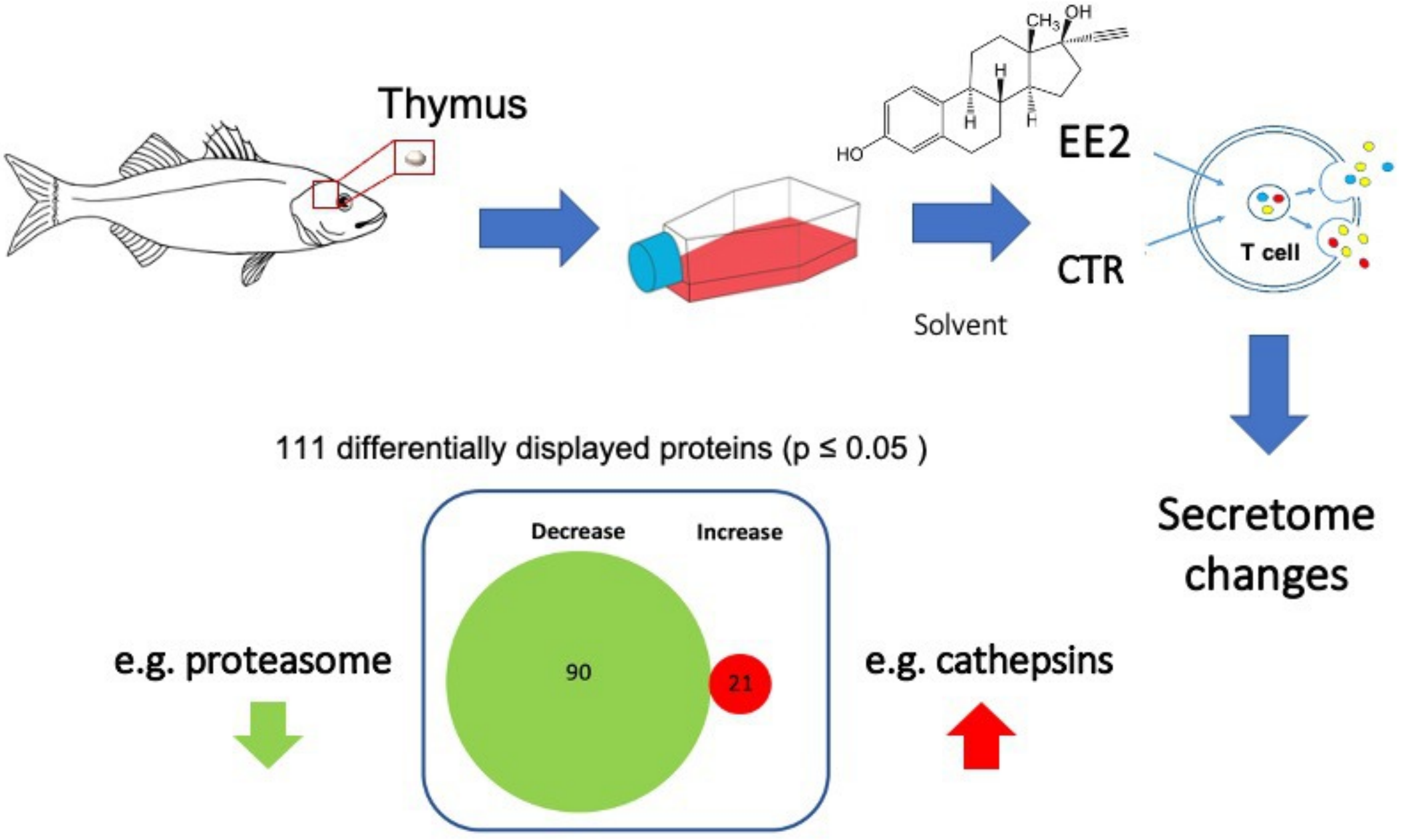
Thymus
EE2
CTR
Solvent
T cell
111 differentially displayed proteins (p ≤ 0.05)
Decrease
Increase
90
21
e.g. proteasome
e.g. cathepsins
Secretome changes